

# Optimal Power Allocation Strategies in Two-Hop X-Duplex Relay Channel

Alessandro Nordin<sup>1</sup>, Member, IEEE, Carla-Fabiana Chiasserini<sup>2</sup>, Fellow, IEEE, and Emanuele Viterbo<sup>3</sup>, Fellow, IEEE

**Abstract**—We consider a dual-hop, decode-and-forward network, where the relay can operate in full-duplex (FD) or half-duplex (HD) mode (X-duplex relay). We model the residual self-interference as an additive Gaussian noise with variance proportional to the relay transmit power, and we assume a Gaussian input distribution at the source. Unlike previous work, we assume that the source is only aware of the transmit power distribution adopted by the relay, but not of the symbols that the relay is currently transmitting. This assumption better reflects the practical situation, where the relay node forwards data traffic but modifies physical-layer or link-layer control information. We then identify the optimal power allocation strategy at the source and relay, which in some cases coincides with the HD transmission mode. We prove that such strategy implies either FD transmissions over an entire time frame or FD/HD transmissions over a variable fraction of the frame. We determine the optimal transmit power level at the source and relay for each frame, or fraction thereof. We compare the performance of our scheme against reference FD and HD techniques, which assume that the source is aware of the symbols instantaneously transmitted by the relay, and show that our solution closely approaches such strategies.

**Index Terms**—Full-duplex, half-duplex, relay networks, communication strategies.

## I. INTRODUCTION

**M**ULTI-HOP relay communications are a key technology for next generation wireless networks, as they can extend radio access in case of coverage holes or users at the cell edge, as well as increase the potentialities of device-to-device data transfers. The dual-hop relay channel, in particular, has been widely investigated under different cooperative schemes, namely, decode-and-forward (DF), compress-and-forward (CF) and amplify-and-forward (AF) [1]–[5]. Most of

this body of work has assumed the relay node to operate in half-duplex (HD) mode. Specifically, results on the capacity of the HD dual-hop relay channel have appeared in [6] and [7], where it was shown that the network capacity is achieved by a discrete input when no direct link between the source and the destination exists.

More recently, a number of studies [8]–[12] have addressed the case where the relay operates in full-duplex (FD) mode, i.e., it can transmit and receive simultaneously on the same frequency band. Indeed, advances in self-interference suppression in FD systems have made such a technology very attractive for relay networks. The capacity of Gaussian two-hop FD relay channels has been characterized in [13], under the assumption that the residual self-interference can be neglected. The more realistic case where residual self-interference ([14], [15]) is taken into account, has been instead addressed in [8]–[12] and [16]–[18]. In these works, the signal looping back from the relay output to its input is modeled as an additive noise with variance proportional to the relay transmit power. In particular, [16] considers an AF relay, which can work in either FD or HD, and derives the distribution of the signal-to-interference plus noise ratio (SINR), the outage probability, and the average rate. The study in [17] compares the performance in terms of block error rate for FD and HD in the case of DF relay, ultra reliable short-packet communication and finite blocklength codes. The work in [8] analyses the instantaneous and average spectral efficiency of a dual-hop network with direct link between source and destination, and a relay node that can operate in either HD or FD mode. Interestingly, the authors propose hybrid FD/HD relaying policies that, depending on the channel conditions, optimally switch between the two operational modes when the FD relay transmit power is fixed to its maximum value, as well as when it can be reduced in order to mitigate self-interference as needed. The FD mode only is considered in [10], which aims to maximize the SINR as the relay transmit power varies, in the case where AF is used, the relay has multiple transmit antennas and a single receive antenna, and constraints on the average and maximum relay transmit power must hold. In [11], the maximum achievable rate and upper bounds on the capacity are obtained when the relay node operates in DF and CF and Gaussian inputs are considered at the source and the relay.

The study in [12] investigates the capacity of the Gaussian two-hop FD relay channel where the residual self-interference is assumed to be a Gaussian random variable with variance

Manuscript received August 30, 2017; revised December 5, 2017 and February 1, 2018; accepted February 25, 2018. Date of publication March 6, 2018; date of current version July 13, 2018. The work was partially supported by Politecnico di Torino through the FLAG project. The work of Emanuele Viterbo was supported by the Australian Research Council Discovery Project under Grant ARC DP160101077. The associate editor coordinating the review of this paper and approving it for publication was Y. Li. (Corresponding author: Alessandro Nordin.)

A. Nordin is with CNR-IEIIT, 10129 Turin, Italy (e-mail: alessandro.nordin@ieiit.cnr.it).

C.-F. Chiasserini is with the Department of Electronics and Telecommunications, Politecnico di Torino, 10129 Turin, Italy, and also with CNR-IEIIT 10129 Turin, Italy (e-mail: chiasserini@polito.it).

E. Viterbo is with the Electrical and Computer Systems Engineering Department, Monash University, Clayton, VIC 3800, Australia (e-mail: emanuele.viterbo@monash.edu).

Color versions of one or more of the figures in this paper are available online at <http://ieeexplore.ieee.org>.

Digital Object Identifier 10.1109/TCOMM.2018.2812707

depending on the amplitude of the transmit symbol of the relay. Also, [12] assumes the average transmit power at source and relay nodes to be limited to some maximum values. The study shows that the optimal conditional probability distribution of the source input, given the relay input, is Gaussian while the optimal distribution of the relay input is either Gaussian or symmetric discrete with finite mass points. This result implies that, under the above assumptions, a capacity achieving scheme requires the source to know at each time instant what the relay is transmitting. This can be realized with the aid of a buffer at the relay, which holds the data previously transmitted by the source and correctly decoded by the relay. The relay re-encodes such data before forwarding it to the destination in the next available channel use. The source can use the same encoder as the relay, in order to predict what will be transmitted by the relay and hence guarantee a capacity achieving transmission.

In this work, we consider a scenario similar to [12], including a dual-hop, DF network where the relay can operate in FD or HD mode (i.e., X-duplex mode), and the residual self-interference is modeled as an additive Gaussian noise, with variance proportional to the relay transmit power. Differently from [12], in this paper we consider the case where the source does not know what symbols are transmitted by the relay at a given time instant and is aware only of the transmit power distribution adopted by the relay over a given time horizon. Thus, our scenario can accommodate the practical case where the relay node, although retransmitting to the destination the same information sent by the source, it may transmit symbols different from those it has received. Examples include the case where the relay modifies physical-layer or link-layer in-band control information, as well as the case where the relay performs link-layer data encryption using a key that is unknown to the source. In this scenario, the source knowledge about the relay power is exploited in order to optimally set the source transmit power and decide whether the relay should operate in HD or FD. Furthermore, we assume a Gaussian input distribution at both source and relay, with variance not exceeding a target maximum value.

Under this scenario, we formulate an optimization problem that aims at maximizing the achievable data rate, subject to the system constraints. We characterize different operational regions corresponding to optimal network performance, and provide conditions for their existence. Our analysis leads to the following major results:

- (i) The distribution of the transmit power at the relay can be conveniently taken as the driving factor toward the network performance optimization. We prove that the optimal probability density function (pdf) of such a quantity is discrete and composed of either one or two delta functions, depending on the target value of average transmit power at the source and relay. We provide the expression of the above distribution for the whole range of the system parameter values, including the channel gains and the target values for the average transmit power at the source and the relay.
- (ii) The above finding leads to the optimal communication strategy for the network under study, which implies

either FD transmissions over an entire frame, or FD/HD transmissions over a fraction of the frame.

- (iii) Given the optimal transmit power distribution at the relay, we derive the optimal power level to be used over time at the relay and the source, i.e., the power allocation policy that yields the system maximum data rate. We remark that our policy establishes the time fractions during which the relay should work in FD and in HD, as well as the transmit power to be used at the source and the relay, given that only the average (not the instantaneous) relay transmit power needs to be known at the source.
- (iv) We compare the results of our optimal power allocation to a reference FD and HD scheme, where the source knows the *instantaneous* relay transmit power. Interestingly, our scheme closely approaches the performance of such strategy in all the considered scenarios.

In the rest of the paper we introduce our system model in Sec. II and we present the constrained optimization problem, along with an overview of the methodology we use in Sec. III. The optimal communication strategy and our main analytical results are presented in Secs. IV and V. Sec. VI shows some performance results, and Sec. VII extends the analysis to a limited average transmission power at the source. Finally, Sec. VIII concludes the paper.

## II. SYSTEM MODEL

We consider a two-hop, DF relay network including a source node  $s$ , a relay  $r$  and a destination  $d$ . All network nodes are equipped with a single antenna, and the relay can work in either FD or HD mode (X-duplex). No direct link exists between source and destination, thus information delivery from the source to the destination necessarily takes place through the relay. As far as the channel is concerned, we consider independent, memoryless block fading channels with additive Gaussian noise, between source and relay as well as between relay and destination.

The source and the relay operate on a *frame* basis, of constant duration  $T$ , with  $T$  being set so that channel conditions do not vary during a frame. In general, the following modes of operations are possible for source and relay: (i) the source transmits while the relay receives only (HD-RX mode); (ii) the source is inactive while the relay transmits (HD-TX mode), (iii) the source transmits while the relay transmits and receives at the same time (FD mode).

We remark, that in our model source and relay do not need to be synchronized on a per-symbol basis, and that the relay can modify link-layer or physical-layer multiple control information as well as perform link-layer data encryption. This implies that, in order to select its operational mode, the source is not required to be aware of the information the relay is transmitting. We assume instead that the source has knowledge of the distribution of the transmit power adopted by the relay across a frame.

When the relay transmits to the destination, a residual self-interference (after analog and digital suppression) adds up to what the relay receives from the source. Then the signals

received at the relay and destination can be written as:

$$y_r = \sqrt{P}h_1x_s + v + n_r; \quad y_d = \sqrt{p}h_2x_r + n_d \quad (1)$$

where

- $h_1$  and  $h_2$  are the complex static channel gains of the source-relay and relay-destination links, respectively. We consider that  $h_1$  is known to the source, and that both  $h_1$  and  $h_2$  are known to the relay. Also, we assume that the communication between nodes is organized in frames of duration  $T$ , with  $T$  being sufficiently smaller than the channel coherence time, so that channel gains can be considered as static during a frame;
- $x_s$  and  $x_r$  are the input symbols transmitted by the source and the relay, respectively. We assume the input at both source and relay to be zero-mean complex Gaussian distributed with unit variance. From (1), we have that the levels of instantaneous power transmitted by source and relay, are  $P|x_s|^2$  and  $p|x_r|^2$ , respectively. In the most general case,  $P$  and  $p$  are time-varying continuous random variables ranging in  $[0, P^{\max}]$  and  $[0, p^{\max}]$ , respectively. Here we assume<sup>1</sup>  $P$  and  $p$  to be independent of  $x_s$  and  $x_r$ , respectively;
- $n_r$  and  $n_d$  represent zero-mean complex Gaussian noise with variance  $N_0$  over the source-relay and the relay-destination link, respectively;
- $v$  represents the instantaneous residual self-interference at the relay. As typically done in previous studies [11], [12], [19], [20], given  $p$ , we model  $v$  as a Gaussian noise with variance proportional to the instantaneous transmission power at the relay, i.e., given  $p$ ,  $v|p \sim \mathcal{N}_{\mathbb{C}}(0, \beta p)$ . In these expressions,  $\beta$  denotes the self-interference attenuation factor at the relay. As shown in [12], assuming  $v$  as a zero-mean i.i.d. Gaussian random variable represents the worst-case linear residual self-interference model.

We also define  $f(p)$  as the probability density function of  $p$ , with support in  $[0, p^{\max}]$ . Finally, we consider that the average power over a frame at the source and at the relay is constrained to given target values, denoted by  $\bar{P}$  and  $\bar{p}$ , respectively. The average transmit power at the source and relay is therefore given by:

$$\bar{p} = \mathbb{E}_p \mathbb{E}_{x_r} [p|x_r|^2] = \mathbb{E}_p [p] = \int_0^{p^{\max}} pf(p) dp \quad (2)$$

$$\bar{P} = \mathbb{E}_p \mathbb{E}_{x_s} [P|x_s|^2] = \mathbb{E}_p [P] = \int_0^{p^{\max}} P(p)f(p) dp \quad (3)$$

where  $\mathbb{E}[\cdot]$  is the average operator and the expression in (3) is due to the fact that the source may select its transmission power based on its knowledge of  $p$ , hence  $P$  can be conveniently described as a function of  $p$ . In order to highlight this dependency, in (3) and in the following,  $P(p)$  indicates the transmit power level at the source when the transmit power level at the relay is set to  $p$ . Moreover, in the following  $P(\cdot)$  indicates the generic function of transmit power allocation at the source, which depends on the relay transmit power. From the definition of the received signals given in (1), assuming

a sufficiently long frame length  $T$ , and having fixed both  $p$  and  $P(p)$ , the rates on the source-relay and relay-destination links are given by  $\log\left(1 + \frac{P(p)|h_1|^2}{N_0 + \beta p}\right)$  and  $\log\left(1 + \frac{p|h_2|^2}{N_0}\right)$ , respectively. Then the average rates achieved over a frame can be written by averaging the above quantities over the random variable  $p$ :

$$R_1(f, P) = \int_0^{p^{\max}} f(p) \log\left(1 + \frac{P(p)|h_1|^2}{N_0 + \beta p}\right) dp;$$

$$R_2(f) = \int_0^{p^{\max}} f(p) \log\left(1 + \frac{p|h_2|^2}{N_0}\right) dp. \quad (4)$$

where we recall that  $p$ , hence also  $P(p)$ , is not a function of the transmitted messages. In (4), by writing  $R_1(f, P)$  and  $R_2(f)$  we highlight that such rates depend on the choice of the power allocation function at the relay,  $f(\cdot)$ , and at the source,  $P(\cdot)$ .

### III. PROBLEM FORMULATION

In our study, we aim at determining the power allocation at the source,  $P(\cdot)$ , and the one at the relay,  $f(\cdot)$ , that maximize the achievable rate of the dual-hop network described above. To this end, we start by recalling some fundamental concepts:

- (a) the network rate will be determined by the minimum between the rate achieved over the source-relay link and over the relay-destination link;
- (b)  $R_1(f, P)$  depends on the source transmit power, the Gaussian noise, and on the residual self-interference at the relay, which, in turn, depends on the relay transmit power;
- (c)  $R_2(f)$  depends on the relay transmit power and the noise at the destination;
- (d) the transmit power at source and relay may vary over time. When  $P(p) > 0$  and  $p > 0$ , the relay is in FD mode, while, when  $P(p) > 0$  and  $p = 0$ , the relay is in HD-RX mode. When  $P(p) = 0$  and  $p > 0$ , the relay is in HD-TX mode and the source is silent.

Based on (b) and (c), the residual self-interference introduces a dependency between the performance of the first and second hop. Under such conditions and under the constraints on the average and the maximum transmit power at the source and at the relay, the maximum rate achievable by the two-hop relay network is defined as

$$R = \max_{f(\cdot)} \min \left\{ \max_{P(\cdot)} R_1(f, P), R_2(f) \right\} \quad (5)$$

where the last equality comes from the fact that only  $R_1(f, P)$  depends on  $P(\cdot)$ . From the definition of  $R$  it is clear that, in order to maximize the network rate, source and relay should coordinate their power allocation strategies. In our study, we optimize such power allocations, hence the source-to-destination rate, by controlling the distribution of the transmit power at the relay,  $f(\cdot)$ , and the distribution of the transmit power at the source,  $P(\cdot)$ .

As a first step, in Section III-A we fix  $f(\cdot)$  and maximize  $R_1$  with respect to  $P(\cdot)$ . By doing so, we rewrite  $R_1$  as a function of, essentially, a Lagrange multiplier,  $\omega$ , and  $f(\cdot)$ . Then, in Section III-B, we formulate the maximization problem over

<sup>1</sup>The transmit power at the source and the relay are denoted by  $P$  (capital letter) and  $p$  (small capital letter).

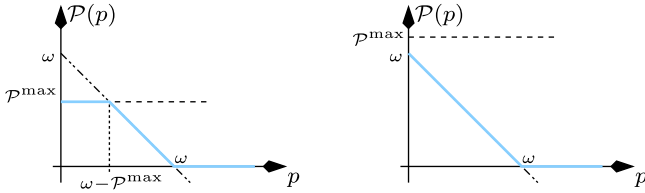


Fig. 1. Transmission power at the source,  $\mathcal{P}(p)$ , for  $\mathcal{P}^{\max} \leq \omega$  (left) and  $\mathcal{P}^{\max} > \omega$  (right).

the  $(\omega, f(\cdot))$  space, which will lead us to find the optimal transmit power distribution at the relay as well as at the source node.

#### A. Optimal Transmit Power Allocation at the Source

For a given distribution  $f(\cdot)$ , in order to maximize the rate  $R_1(f, P)$  with respect to  $P(\cdot)$  we need to solve the following problem

$$\mathbf{P0}: R_1(f) = \max_{P(\cdot)} R_1(f, P) \quad \text{s.t.}$$

$$(a) \int_0^{\mathcal{P}^{\max}} P(p) f(p) dp = \bar{P}; \quad (b) 0 \leq P(p) \leq \mathcal{P}^{\max}$$

where (a) represents the constraint on the source average transmit power given by (3) and (b) is the constraints on the maximum source transmit power. Problem **P0** can be solved using calculus of variations techniques. Specifically, it can be shown (see Appendix A) that, given  $f(\cdot)$ , the maximizer of **P0** is given by

$$P(p) = \frac{\beta}{|h_1|^2} \min \{ [\omega - p]^+, \mathcal{P}^{\max} \} \quad (6)$$

where  $[\cdot]^+ \triangleq \max\{0, \cdot\}$ ,  $\mathcal{P}^{\max} \triangleq P^{\max} |h_1|^2 / \beta$  and  $\omega$  is a parameter defined as (see Appendix A):  $\omega \triangleq \frac{|h_1|^2}{\beta \lambda} - \frac{N_0}{\beta}$  with  $\lambda$  being the Lagrange multiplier used in the constrained maximization of  $R_1(f, P)$ . Given  $f(\cdot)$ , the value of  $\omega$  can be obtained by substituting (6) into the constraint **P0**-(a). The function  $\mathcal{P}(p) \triangleq \min \{ [\omega - p]^+, \mathcal{P}^{\max} \}$ , proportional to (6), is plotted in Fig. 1 (blue line) for the cases  $\mathcal{P}^{\max} \leq \omega$  (left) and  $\mathcal{P}^{\max} > \omega$  (right).

In particular, we observe that when  $P^{\max}$  is sufficiently large, the optimal power allocation at the source behaves as depicted in Fig. 1(right) and it can be simplified to

$$P(p) = \frac{\beta}{|h_1|^2} [\omega - p]^+. \quad (7)$$

This scenario encompasses the case where the source is a macro-cell base-station (BS) and the relay is a small-cell BS, with the macro-cell BS having weaker constraints on the maximum transmit power than the small-cell BS. The case where instead the value of  $P^{\max}$  is smaller than  $\omega$ , is more complicated to deal with (see Fig. 1(left)). This case encompasses the situation where the source is a user equipment transmitting to a small-cell BS, which relays traffic toward a macro-cell BS.

In the following, in order to simplify the derivation of the network rate, we assume  $P^{\max}$  to be sufficiently large; we will

remove this assumption in Sec. VII, where we briefly explain how to solve the problem when the parameter  $P^{\max}$  comes into play. Then, by substituting (7) in constraint **P0**-(a) and in the expression for  $R_1(f, P)$  in (4), we obtain, respectively,

$$\int_0^{\mathcal{P}^{\max}} f(p) [\omega - p]^+ dp = \bar{P} \frac{|h_1|^2}{\beta} \triangleq \bar{\mathcal{P}} \quad (8)$$

$$R_1(f) = \int_0^{\mathcal{P}^{\max}} f(p) \times \log \left( 1 + \frac{\beta_0 [\omega - p]^+}{1 + \beta_0 p} \right) dp, \quad (9)$$

where  $\beta_0 \triangleq \frac{\beta}{N_0}$ . Thus, we now have both the rate  $R$ , optimized with respect to  $P(\cdot)$  and the constraint on the average source power, expressed as functions of the parameter  $\omega$ .

#### B. Rate Maximization Problem

After having optimized the source transmit power, we need to find the optimal distribution  $f(\cdot)$  that maximizes the network data rate  $R$ , as indicated in (5). To this end, we formulate the following optimization problem, subject to the system constraints:

$$\mathbf{P1}: R = \max_{f(\cdot)} \min \{ R_1(f), R_2(f) \} \quad \text{s.t.}$$

$$(a) R_1(f) = \int_0^{\mathcal{P}^{\max}} f(p) \log \left( 1 + \frac{\beta_0 [\omega - p]^+}{1 + \beta_0 p} \right) dp$$

$$(b) R_2(f) = \int_0^{\mathcal{P}^{\max}} f(p) \log(1 + vp) dp$$

$$(c) \int_0^{\mathcal{P}^{\max}} f(p) [\omega - p]^+ dp = \bar{\mathcal{P}}$$

$$(d) \int_0^{\mathcal{P}^{\max}} pf(p) dp = \bar{p}; \quad \int_0^{\mathcal{P}^{\max}} f(p) dp = 1; \quad 0 \leq p \leq \mathcal{P}^{\max}$$

where  $v \triangleq \frac{|h_2|^2}{N_0}$  in (b). In the above formulation, (a) represents the average rate achieved over a frame on the source-relay link in (9); (b) represents the average rate achieved over a frame on the relay-destination link in (4); (c) is the average power constraint at the source specified in (8); (d) imposes that the mean value of transmit power at the relay equals  $\bar{p}$ , that  $f(\cdot)$  is a distribution, and that  $p$  does not exceed  $\mathcal{P}^{\max}$ .

If  $f(\cdot)$  were known, constraint **P1**-(c) would completely determine the parameter  $\omega$ . However, this is not the case in our scenario; in fact,  $f(\cdot)$  is the function that we need to properly select to maximize the source-to-destination rate. It follows that, in general, in our problem  $\omega$  is a free parameter and we need to maximize the rate over the  $(\omega, f(\cdot))$  space. An overview of the methodology we adopt to solve such a problem is provided below.

#### C. Roadmap

We consider the following two cases:  $\omega \geq \mathcal{P}^{\max}$  (Sec. IV) and  $\omega < \mathcal{P}^{\max}$  (Sec. V). While the former can be handled analytically by directly addressing the above problem formulation, the latter is far more complicated and requires the definition of a novel methodology. Specifically,



(i) for  $\omega \geq p^{\max}$ , we first find lower and upper bounds for  $R_1(f)$  and  $R_2(f)$  so that three different cases can be identified. For all of them, we obtain the optimal transmit power allocation at the source and relay. The third of these cases leads to a particularly interesting result, which shows that the network rate is maximized when  $f(p)$  is discrete with one or two probability masses, depending on the value of the system parameters (e.g., channel gains and self-interference mitigation factor). As by-product of this analysis, we also obtain the optimal communication scheme, which turns out to be a time-division strategy;

(ii) for  $\omega < p^{\max}$ , we show that the rate maximization problem can be rewritten in a simpler form by expressing  $f(p)$  as the sum of two distributions with support over two distinct intervals of values of  $p$ . The simpler formulation we get allows bounding the rates on the two links, and analysing the expressions for the two rates over different sub-regions of the solution space. Also, we can provide analytical solutions for the network rate, and the optimal power allocation and transmit strategy at the relay and at the source.

Our main analytical results are summarized in Tables I and II.

#### IV. OPTIMAL POWER ALLOCATION FOR $\omega \geq p^{\max}$

We solve the problem **P1** by first considering the case  $\omega \geq p^{\max}$ , which allows to remove the  $[\cdot]^+$  operator in constraint **P1-(a)** and **P1-(c)**. This case was also sketched in our conference paper [21]. Then, by using the equalities provided in **P1-(d)** in **P1-(c)**, we obtain  $\omega = \bar{P} + \bar{p}$ . By plugging such expression for  $\omega$  in **P1-(a)** and in (7), we get

$$R_1(f) = \log(1 + \beta_0(\bar{P} + \bar{p})) - \int_0^{p^{\max}} f(p) \log(1 + \beta_0 p) dp \quad (10)$$

and, from (9)  $P(p) = \frac{\beta}{|h_1|^2}[\bar{P} + \bar{p} - p]$ . Moreover, since  $\omega = \bar{P} + \bar{p}$ , the constraint  $\omega \geq p^{\max}$  implies  $\bar{P} \geq p^{\max} - \bar{p} \triangleq \mathcal{P}_0$  where we recall that  $\bar{P} \triangleq \bar{P} \frac{|h_1|^2}{\beta}$ . In this section, we analyze the behavior of the system for  $\bar{P} \geq \mathcal{P}_0$ .

In order to solve problem **P1**, as a first step we provide upper and lower bounds to  $R_1(f)$  and  $R_2(f)$  (Sec. IV-A). Such bounds are then used to identify three possible cases, in each of which we solve **P1** to the optimum (Sec. IV-B).

##### A. Bounding $R_1(f)$ and $R_2(f)$

Let us consider  $R_1(f)$  and  $R_2(f)$ , as given, respectively, in (10) and in constraint **P1-(b)**; an upper and a lower bound to such expressions can be obtained through the lemma below.

*Lemma 1:* Let  $\phi(p)$  be a continuous concave function and  $f(p)$  be a probability distribution, both with support in  $[a, b]$ . Let  $\int_a^b pf(p) dp = m$ . Then,

$$\frac{b-m}{b-a}\phi(a) + \left(1 - \frac{b-m}{b-a}\right)\phi(b) \leq \int_a^b f(p)\phi(p) dp \leq \phi(m).$$

The lower bound holds with equality when  $f(p) = \frac{b-m}{b-a}\delta(p-a) + \left(1 - \frac{b-m}{b-a}\right)\delta(p-b)$ , while the upper bound holds with equality when  $f(p) = \delta(p-m)$ , where  $\delta(\cdot)$  is the Dirac delta.

*Proof:* The proof is reported in Appendix B. ■

We observe that the term  $\log(1 + cp)$ ,  $c > 0$ , appearing as argument of the integrals in (10) and **P1-(b)**, is a concave function of  $p$ . Since  $f(p)$  is a distribution with average  $\bar{p}$ , we can exploit the lower bound provided by Lemma 1 and write:

$$R_1 \leq \log(1 + \beta_0(\bar{P} + \bar{p})) - \frac{\bar{p}}{p^{\max}} \log(1 + \beta_0 p^{\max}) \triangleq r_1^{\max} \quad (11)$$

$$R_2 \geq \frac{\bar{p}}{p^{\max}} \log(1 + v p^{\max}) \triangleq r_2^{\min} \quad (12)$$

with the equality in (11) and (12) holding when  $f(p) = \left(1 - \frac{\bar{p}}{p^{\max}}\right)\delta(p) + \frac{\bar{p}}{p^{\max}}\delta(p - p^{\max})$ . Similarly, by applying the upper bound provided by Lemma 1, we get:

$$\begin{aligned} R_1 &\geq \log(1 + \beta_0(\bar{P} + \bar{p})) - \log(1 + \bar{p}\beta_0) \triangleq r_1^{\min}; \\ R_2 &\leq \log(1 + \bar{p}v) \triangleq r_2^{\max} \end{aligned} \quad (13)$$

with the equality holding when  $f(p) = \delta(p - \bar{p})$ .

##### B. Solving **P1**

The bounds to  $R_1(f)$  and  $R_2(f)$ , in Section IV-A, allow us to break problem **P1** into three cases, as detailed below.

1) If  $r_2^{\min} \geq r_1^{\max}$ , then  $R = r_1^{\max}$  and the optimal relay power distribution is  $f^*(p) = \left(1 - \frac{\bar{p}}{p^{\max}}\right)\delta(p) + \frac{\bar{p}}{p^{\max}}\delta(p - p^{\max})$ . Solving for  $\bar{P}$  the inequality  $r_2^{\min} \geq r_1^{\max}$ , we obtain

$$\begin{aligned} \bar{P} &\leq \mathcal{P}_1 \triangleq \frac{1}{\beta_0} [(1 + p^{\max}\beta_0)(1 + p^{\max}v)]^{\frac{\bar{p}}{p^{\max}}} - \frac{1 + \bar{p}\beta_0}{\beta_0} \\ R &= \log(1 + \beta_0(\bar{P} + \bar{p})) - \frac{\bar{p}}{p^{\max}} \log(1 + \beta_0 p^{\max}). \end{aligned}$$

2) If  $r_1^{\min} \geq r_2^{\max}$ , then  $R = r_2^{\max}$  and the optimal relay power distribution is  $f^*(p) = \delta(p - \bar{p})$ . Solving for  $\bar{P}$  the inequality  $r_1^{\min} \geq r_2^{\max}$ , we get

$$\bar{P} \geq \mathcal{P}_2 \triangleq \bar{p}v \frac{1 + \bar{p}\beta_0}{\beta_0}; \quad R = \log(1 + \bar{p}v).$$

3) Otherwise, we find solutions for  $f(\cdot)$  such that  $R = R_1 = R_2$ . Indeed, for  $\mathcal{P}_1 \leq \bar{P} \leq \mathcal{P}_2$ , problem **P1** becomes:

$$\mathbf{P2:} \quad R = \log(1 + \beta_0(\bar{P} + \bar{p}))$$

$$- \min_{f(\cdot)} \int_0^{p^{\max}} f(p) \log(1 + \beta_0 p) dp \quad \text{s.t.}$$

$$(a) \quad \int_0^{p^{\max}} f(p) \log[(1 + p\beta_0)(1 + pv)] dp = \log(1 + \beta_0(\bar{P} + \bar{p}))$$

$$(b) \quad \int_0^{p^{\max}} pf(p) dp = \bar{p}; \quad (c) \quad \int_0^{p^{\max}} f(p) dp = 1.$$

The minimizer of the functional can be found by applying the theorem below, which shows that the solution of optimization problems such **P2** is given by one or two delta functions, depending on the value of the parameters appearing in the problem formulation.

**Theorem 2:** Consider the following constrained minimization problem:

$$\begin{aligned} \min_{f(\cdot)} \int_a^b f(p)\phi(p) dp \quad \text{s.t.} \\ (a) \int_a^b f(p)\psi(p) dp = c; \quad (b) \int_a^b pf(p) dp = m \\ (c) \int_a^b f(p) dp = 1; \quad (d) f(p) \geq 0, \forall p \in [a, b]; \end{aligned} \quad (14)$$

where  $\phi(p) = \log(1 + \gamma_1 p)$ ,  $\eta(p) = \log(1 + \gamma_2 p)$ ,  $\psi(p) = \phi(p) + \eta(p)$ , and  $f(p)$  is a probability distribution with support in  $[a, b]$ ,  $a > 0$ . Moreover,  $\gamma_1 > 0$ ,  $\gamma_2 > 0$ ,  $m \in [a, b]$  and  $c$  are constant parameters. Then, the minimizer has the following expression

$$f^*(p) = \begin{cases} \frac{p_2 - m}{p_2 - a} \delta(p - a) + \frac{m - a}{p_2 - a} \delta(p - p_2) & \text{if } \gamma_1 > \gamma_2 \\ \frac{b - m}{b - p_1} \delta(p - p_1) + \frac{m - p_1}{b - p_1} \delta(p - b) & \text{if } \gamma_1 \leq \gamma_2 \end{cases} \quad (15)$$

where  $p_1 \in [a, m]$  and  $p_2 \in [m, b]$  are obtained by replacing (15) in the constraint (a) in (14).

*Proof:* The proof is given in Appendix D.  $\blacksquare$

Through Theorem 2 and considering  $v \geq \beta_0$ , the maximizer of the rate in **P2** is:

$$f^*(p) = \frac{p^{\max} - \bar{p}}{p^{\max} - p_1} \delta(p - p_1) + \frac{\bar{p} - p_1}{p^{\max} - p_1} \delta(p - p^{\max}) \quad (16)$$

where  $p_1$  is obtained by replacing  $f(p)$  with (16) in constraint **P2**-(a), i.e., by solving the following equation for  $p_1$

$$\left[ \frac{(1 + p_1 \beta_0)(1 + p_1 v)}{k} \right]^{\frac{p^{\max} - \bar{p}}{p^{\max} - p_1}} = \frac{1 + \beta_0(\bar{P} + \bar{p})}{k} \quad (17)$$

with  $k = (1 + p^{\max} \beta_0)(1 + p^{\max} v)$ . When  $v < \beta_0$ , the maximizer of the rate in **P2** is

$$f^*(p) = \frac{p_2 - \bar{p}}{p_2} \delta(p) + \frac{\bar{p}}{p_2} \delta(p - p_2) \quad (18)$$

where  $p_2$  is obtained using  $f^*(p)$  in **P2**-(a), i.e., by solving the following equation for  $p_2$

$$[(1 + p_2 \beta_0)(1 + p_2 v)]^{\frac{\bar{p}}{p_2}} = 1 + \beta_0(\bar{P} + \bar{p}). \quad (19)$$

Given the optimal distribution  $f^*(p)$ , which represents the optimal transmit power allocation at the relay, the optimal power allocation at the source node can be obtained by using (7). From the implementation view point, such a scheme implies minimal overhead since  $f^*(p)$  is composed of one or two  $\delta$  functions. Thus, it is enough that the sends to the source the parameters of such  $\delta$ 's. It is however important that source and relay are synchronized at the frame level.

From the above results, important observations can be made:

- (i) the power allocation at the relay that leads to the maximum rate depends on the channel gain  $h_2$  through  $v$  (see (16) and (18) where  $p_1$  and  $p_2$ , given in (17)

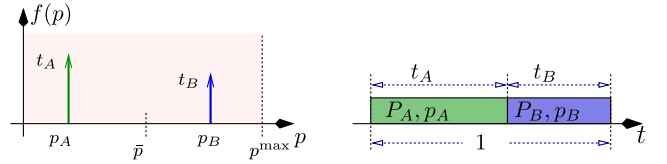


Fig. 2. Left: Optimal communication strategy during a frame resulting in two phases (A and B). Right: Optimal distribution of the average relay transmit power at the relay ( $p$ ).

and (19), depend on  $v$ ). Similarly, the power allocation at the source depends on channel gain  $h_1$  (see (7));

- (ii) more importantly, the optimal power allocation  $f^*(p)$  at the relay is *discrete*, with either one or two probability masses depending on the number of  $\delta$  functions appearing in the expression of  $f^*(p)$ ;
- (iii) the above finding implies that source and relay should operate according to a time division strategy consisting of transmissions over either the entire frame (when  $f^*(p)$  includes one probability mass only), or two fractions of the frame (when two probability masses appear in  $f^*(p)$ ). We will refer to such fractions as, respectively, phase A and phase B; clearly, they reduce to one phase when  $f^*(p)$  includes only one probability mass. An example where two phases exist is depicted in Fig. 2(left);
- (iv) The phases duration are given by the coefficients of the  $\delta$  functions composing  $f^*(p)$  (see Fig. 2(right)). Note that now  $p$  takes on a new meaning, as it represents the average level of transmission power to be used at the relay during a frame phase. The values of  $p$ , hence of the relay average transmission power over each phase, are given by the arguments of the  $\delta$ 's in  $f^*(p)$ . Likewise, through (7), the average level of transmitted power at the source is determined by the arguments of the  $\delta$  functions in  $f^*(p)$ .

To summarize, Table I reports the solution of problem **P1** for  $\bar{P} \geq P_0$ , along with the corresponding power allocation at the source and relay. Thus the two tables also specify the optimal communication strategy at source and relay, i.e.,

- for  $\bar{P} \leq P_1$ , both source and relay transmit during phase A and thus the relay operates in FD. In phase B, the relay is silent and only receives (HD-RX mode);
- for  $\bar{P} \in (P_1, P_2)$ , two cases are possible. For  $v \geq \beta_0$  the relay always operates in FD but source and relay use different power levels in the two phases. Otherwise, the relay uses the same scheme as for  $\bar{P} \leq P_1$ , i.e., FD in phase A and HD-RX in phase B, but its transmit power in phase A should be set to  $p_2$ ;
- for  $\bar{P} \geq P_2$ , the relay continuously operates in FD over the entire frame, and source and relay always transmit at their average power.

## V. OPTIMAL POWER ALLOCATION FOR $\omega < p^{\max}$

In this section, we solve problem **P1** when  $\omega < p^{\max}$ . To this end, we first show that **P1** can be recast in a simpler

TABLE I  
OPTIMAL POWER ALLOCATION AND RATE FOR  $\bar{\mathcal{P}} \geq \mathcal{P}_0$ .  $t_A$  AND  $t_B = 1 - t_A$  ARE THE TIME FRACTIONS REPRESENTING THE PHASES DURATION. THE PHASES IN WHICH THE RELAY WORKS IN HD ARE SHADED

$v \geq \beta_0$	Phase A			Phase B		
	$t_A$	$P_A$	$p_A$	$t_B$	$P_B$	$p_B$
$\bar{\mathcal{P}} \in [\mathcal{P}_0, \mathcal{P}_1]$	$\frac{\bar{p}}{p^{\max}}$	$\frac{\beta}{ h_1 ^2}(\bar{\mathcal{P}} + \bar{p} - p^{\max})$	$p^{\max}$	$1 - \frac{\bar{p}}{p^{\max}}$	$\frac{\beta}{ h_1 ^2}(\bar{\mathcal{P}} + \bar{p})$	0
$\bar{\mathcal{P}} \in (\mathcal{P}_1, \mathcal{P}_2)$	$\frac{\bar{p}-p_1}{p^{\max}-p_1}$	$\frac{\beta}{ h_1 ^2}(\bar{\mathcal{P}} + \bar{p} - p^{\max})$	$p^{\max}$	$\frac{p^{\max}-\bar{p}}{p^{\max}-p_1}$	$\frac{\beta}{ h_1 ^2}(\bar{\mathcal{P}} + \bar{p} - p_1)$	$p_1$
$\bar{\mathcal{P}} \in [\mathcal{P}_2, \infty)$	-	-	-	1	$\frac{\beta}{ h_1 ^2}\bar{\mathcal{P}}$	$\bar{p}$
$v < \beta_0$	Phase A			Phase B		
	$t_A$	$P_A$	$p_A$	$t_B$	$P_B$	$p_B$
$\bar{\mathcal{P}} \in [\mathcal{P}_0, \mathcal{P}_1]$	$\frac{\bar{p}}{p^{\max}}$	$\frac{\beta}{ h_1 ^2}(\bar{\mathcal{P}} + \bar{p} - p^{\max})$	$p^{\max}$	$1 - \frac{\bar{p}}{p^{\max}}$	$\frac{\beta}{ h_1 ^2}(\bar{\mathcal{P}} + \bar{p})$	0
$\bar{\mathcal{P}} \in (\mathcal{P}_1, \mathcal{P}_2)$	$\frac{\bar{p}}{p_2}$	$\frac{\beta}{ h_1 ^2}(\bar{\mathcal{P}} + \bar{p} - p_2)$	$p_2$	$1 - \frac{\bar{p}}{p_2}$	$\frac{\beta}{ h_1 ^2}(\bar{\mathcal{P}} + \bar{p})$	0
$\bar{\mathcal{P}} \in [\mathcal{P}_2, \infty)$	1	$\frac{\beta}{ h_1 ^2}\bar{\mathcal{P}}$	$\bar{p}$	-	-	-
Rate $R$						
$\bar{\mathcal{P}} \in [\mathcal{P}_0, \mathcal{P}_1]$	$\log(1 + \beta_0(\bar{\mathcal{P}} + \bar{p})) - \frac{\bar{p}}{p^{\max}} \log(1 + p^{\max}\beta_0)$					
$\bar{\mathcal{P}} \in (\mathcal{P}_1, \mathcal{P}_2); v \geq \beta_0$	$\log(1 + \beta_0(\bar{\mathcal{P}} + \bar{p})) - \frac{p^{\max}-\bar{p}}{p^{\max}-p_1} \log(1 + p_1\beta_0) - \frac{\bar{p}-p_1}{p^{\max}-p_1} \log(1 + p^{\max}\beta_0)$					
$\bar{\mathcal{P}} \in (\mathcal{P}_1, \mathcal{P}_2); v < \beta_0$	$\log(1 + \beta_0(\bar{\mathcal{P}} + \bar{p})) - \frac{\bar{p}}{p_2} \log(1 + p_2\beta_0)$					
$\bar{\mathcal{P}} \in [\mathcal{P}_2, \infty)$	$\log(1 + \bar{p}v)$					

form by rewriting the distribution  $f(p)$  as a sum of two distributions (Sec. V-A). Next, we bound the rates  $R_1(f)$  and  $R_2(f)$  (Sec. V-B) and show that such bounds can be used to break the maximization problem into easier sub-problems, (Secs. V-C and V-D). The expression of the maximum achievable rate is then derived by solving the obtained sub-problems as  $P^{\max}$  varies (Sec. V-E).

A. Rewriting the Maximization Problem in a Simpler Form

We observe that, due to the presence of the  $[\cdot]^+$  operator, the arguments of the constraints **P1-(a)** and **P1-(c)** are identically zero for  $p \in (\omega, p^{\max}]$ , while they can take values greater than zero for  $p \in (0, \omega]$ . This suggests that, given  $\omega \in [0, p^{\max})$ , we can rewrite the distribution  $f(p)$  as the weighted sum of two distributions:  $g(p)$  with support in  $[0, \omega]$ , and  $h(p)$  with support in  $(\omega, p^{\max}]$ ; i.e.,

$$f(p) = F(\omega)g(p) + [1 - F(\omega)]h(p) \tag{20}$$

where  $F(\omega) \in [0, 1]$  is the cumulative distribution function of  $f(p)$ , given by  $F(\omega) = \int_0^\omega f(p) dp$ . It is easy to check that the expression for  $f(p)$  given in (20) integrates to 1 in the range  $[0, p^{\max}]$ . Then constraint **P1-(d)** on the average transmit power at the relay can be rewritten as

$$\bar{p} = F(\omega) \int_0^\omega pg(p) dp + [1 - F(\omega)] \int_\omega^{p^{\max}} ph(p) dp. \tag{21}$$

If we define,

$$\int_0^\omega pg(p) dp \triangleq \frac{G(\omega)}{F(\omega)}, \tag{22}$$

from (21) it immediately follows that

$$\int_\omega^{p^{\max}} ph(p) dp = \frac{\bar{p} - G(\omega)}{1 - F(\omega)} \tag{23}$$

where, being (22) and (23) positive, we have:  $0 \leq G(\omega) \leq \bar{p}$ .

For simplicity, from now on we drop the dependence on  $\omega$  from  $F(\omega)$  and  $G(\omega)$ . The relation between  $F$  and  $G$  can be found by applying the definitions in (20) and (22) to the constraint **P1-(c)**. Doing so, we obtain

$$\int_0^{p^{\max}} f(p)[\omega - p]^+ dp = \int_0^\omega (\omega - p)Fg(p) dp = F\omega - G = \bar{\mathcal{P}} \tag{24}$$

i.e.,  $G = F\omega - \bar{\mathcal{P}}$ . We also need to impose that the averages in (22) and (23) lie within the support of the distributions  $g(p)$  and  $h(p)$ , respectively, i.e.,

$$0 \leq \frac{G}{F} \leq \omega; \quad \omega < \frac{\bar{p} - G}{1 - F} \leq p^{\max}. \tag{25}$$

As shown in Appendix C, recalling that  $\omega \in [0, p^{\max})$ ,  $F \in [0, 1]$ ,  $0 \leq G \leq \bar{p}$  and using (24), the inequalities in (25) define a region  $\Omega \subset \mathbb{R}^2$  of approximately triangular shape given by

$$\Omega = \left\{ (\omega, F) \in \mathbb{R}^2 \left| \begin{aligned} &\frac{p^{\max}\bar{\mathcal{P}}}{p^{\max} - \bar{p}} \leq \omega \leq \bar{\mathcal{P}} + \bar{p}, \\ &\frac{\bar{\mathcal{P}}}{\omega} \leq F \leq \frac{p^{\max} - \bar{p} - \bar{\mathcal{P}}}{p^{\max} - \omega} \end{aligned} \right. \right\} \tag{26}$$

with vertices  $V_1 = \left(\frac{p^{\max}\bar{\mathcal{P}}}{p^{\max} - \bar{p}}, 1 - \frac{\bar{p}}{p^{\max}}\right)$ ;  $V_2 = (\bar{\mathcal{P}} + \bar{p}, 1)$ ;  $V_3 = \left(\bar{\mathcal{P}} + \bar{p}, \frac{\bar{\mathcal{P}}}{\bar{\mathcal{P}} + \bar{p}}\right)$ . Such region exists if  $\bar{\mathcal{P}} < \mathcal{P}_0$  where we recall that  $\mathcal{P}_0 = p^{\max} - \bar{p}$ . The region  $\Omega$  is depicted in Fig. 3(top), where the edge  $V_1$ - $V_2$  has equation  $F = \frac{p^{\max} - \bar{p} - \bar{\mathcal{P}}}{p^{\max} - \omega}$  while the edge  $V_1$ - $V_3$  has equation  $F = \frac{\bar{\mathcal{P}}}{\omega}$ .

Next, we substitute (20) in the the rates  $R_1(f)$  and  $R_2(f)$  given in **P1-(a)** and **P1-(b)**, respectively, and obtain:  $R_1(f) = F \log(1 + \beta_0\omega) - F \int_0^\omega g(p) \log(1 + p\beta_0) dp \triangleq R_1(g)$

and

$$\begin{aligned}
 R_2(f) &= F \int_0^\omega g(p) \log(1 + pv) dp \\
 &\quad + (1 - F) \int_\omega^{p^{\max}} h(p) \log(1 + pv) dp \\
 &\leq F \int_0^\omega g(p) \log(1 + pv) dp \\
 &\quad + (1 - F) \log\left(1 + v \frac{\bar{p} - F\omega + \bar{P}}{1 - F}\right) \\
 &\triangleq \tilde{R}_2(g)
 \end{aligned} \tag{27}$$

where the inequality in (27) follows from Lemma 1 and (23). By writing  $R_1(g)$  and  $\tilde{R}_2(g)$ , we stress the fact that they depend on the distribution  $g(\cdot)$ . The upper bound,  $\tilde{R}_2(g)$ , is achieved for

$$h(p) = \delta\left(p - \frac{\bar{P} + \bar{p} - \omega}{1 - F} - \omega\right). \tag{28}$$

It turns out that, by writing  $f(p)$  as in (20), the maximization problem **P1** reduces to the maximization of the rate  $R$  over  $g(\cdot)$  and over the region  $\Omega$ . Thus, **P1** is recast as

$$\begin{aligned}
 \mathbf{P3}: \quad R &= \max_{g(\cdot), (\omega, F) \in \Omega} \min\{R_1(g), \tilde{R}_2(g)\} \text{ s.t.} \\
 (a) \quad R_1(g) &= F \log(1 + \beta_0 \omega) - F \int_0^\omega g(p) \log(1 + p\beta_0) dp \\
 (b) \quad \tilde{R}_2(g) &= F \int_0^\omega g(p) \log(1 + pv) dp \\
 &\quad + (1 - F) \log\left(1 + v \frac{\bar{P} + \bar{p} - F\omega}{1 - F}\right) \\
 (c) \quad \int_0^\omega pg(p) dp &= \omega - \frac{\bar{P}}{F}; \quad (d) \quad \int_0^\omega g(p) dp = 1
 \end{aligned} \tag{29}$$

where **P3**-(c) is obtained by using (22) and (24), **P3**-(d) states that  $g(p)$  is a pdf.

### B. Bounding the Rates $R_1(g)$ and $\tilde{R}_2(g)$

To solve **P3**, we first apply Lemma 1 to  $R_1(g)$  and  $\tilde{R}_2(g)$ . We obtain:

$$R_1(g) \geq F \log \frac{F(1 + \omega\beta_0)}{F(1 + \omega\beta_0) - \bar{P}\beta_0} \triangleq R_1^{\min} \tag{30}$$

$$\begin{aligned}
 \tilde{R}_2(g) &\leq F \log\left(1 + v \left(\omega - \frac{\bar{P}}{F}\right)\right) \\
 &\quad + (1 - F) \log\left(1 + v \frac{\bar{P} + \bar{p} - F\omega}{1 - F}\right) \triangleq \tilde{R}_2^{\max}.
 \end{aligned} \tag{31}$$

The bounds in (30) and (31) hold with equality when

$$g(p) = \delta\left(p - \omega + \frac{\bar{P}}{F}\right). \tag{32}$$

Similarly, we can write

$$R_1(g) \leq \frac{\bar{P}}{\omega} \log(1 + \beta_0 \omega) \triangleq R_1^{\max} \tag{33}$$

$$\begin{aligned}
 \tilde{R}_2(g) &\geq \left(F - \frac{\bar{P}}{\omega}\right) \log(1 + v\omega) \\
 &\quad + (1 - F) \log\left(1 + v \frac{\bar{P} + \bar{p} - F\omega}{1 - F}\right) \\
 &\triangleq \tilde{R}_2^{\min}.
 \end{aligned} \tag{34}$$

In (33) and (34), equality holds for

$$g(p) = \frac{\bar{P}}{F\omega} \delta(p) + \left(1 - \frac{\bar{P}}{F\omega}\right) \delta(p - \omega). \tag{35}$$

In the following, we use the above bounds to divide the solution space  $\Omega$  into subregions, over which maximizing  $R$  becomes easier.

### C. Breaking the Solution Space Into Subregions

In order to maximize the rate over  $\Omega$ , we exploit the bounds in (30), (31), (33), (34) and define the following subsets of  $\Omega$ .

1)  $\Omega_1 = \left\{(\omega, F) \in \Omega \mid R_1^{\min} \geq \tilde{R}_2^{\max}\right\}$ . Then in  $\Omega_1$  the problem **P3** reduces to maximizing  $\tilde{R}_2^{\max}$ . The maximum rate achieved in  $\Omega_1$  will be denoted by  $R_{\Omega_1}$ . We observe that  $\Omega_1$  can be viewed as the set of points where  $Q_1(\omega, F) \triangleq R_1^{\min} - \tilde{R}_2^{\max} \geq 0$  (i.e.,  $R_1^{\min} \geq \tilde{R}_2^{\max}$ ). Then the implicit curve  $Q_1(\omega, F) = 0$  is one of the edges of  $\Omega_1$  (see Fig. 3(top)). Also, the intersection point between  $Q_1(\omega, F) = 0$  and the edge  $V_1$ - $V_3$ , whose equation is  $F = \frac{\bar{P}}{\omega}$ , is  $A = \left(\omega_A, F_A = \frac{\bar{P}}{\omega_A}\right)$ . The value of  $\omega_A$  can be computed numerically by solving  $Q_1(\omega_A, F_A) = 0$ .

The intersection between  $Q_1(\omega, F) = 0$  and the edge  $V_1$ - $V_2$ , whose equation is  $F = \frac{p^{\max} - \bar{p} - \bar{P}}{p^{\max} - \omega}$ , is  $B = \left(\omega_B, F_B = \frac{p^{\max} - \bar{p} - \bar{P}}{p^{\max} - \omega_B}\right)$ . The value of  $\omega_B$  can be computed numerically by solving  $Q_1(\omega_B, F_B) = 0$ . Moreover, as shown in Appendix E, the curve  $Q_1(\omega, F)$  intersects the line  $\omega = \bar{p} + \bar{P}$  at most in a single point. Finally, it can be seen that  $R_1^{\min}$  decreases with  $\omega$  while  $\tilde{R}_2^{\max}$  increases with  $\omega$  (details can be found in [22]). Thus, we conclude that  $\Omega_1$  is located on the left of the curve  $Q_1(\omega, F) = 0$  (see Fig. 3(top)).

2) Let  $\Omega_2 = \left\{(\omega, F) \in \Omega \mid \tilde{R}_2^{\min} \geq R_1^{\max}\right\}$ . Then in  $\Omega_2$  the problem **P3** reduces to maximizing  $R_1^{\max}$ . The maximum rate achieved in this subregion will be denoted by  $R_{\Omega_2}$ . We observe that  $\Omega_2$  is given by the set of points  $(\omega, F)$  where  $Q_2(\omega, F) \triangleq \tilde{R}_2^{\min} - R_1^{\max} \geq 0$  (i.e.,  $\tilde{R}_2^{\min} \geq R_1^{\max}$ ). Then the implicit curve  $Q_2(\omega, F) = 0$  is one of the edges of  $\Omega_2$ . Also, it can be easily shown that  $R_1^{\max}$  decreases with  $\omega$ , while  $\tilde{R}_2^{\min}$  increases with  $\omega$  and decreases with  $F$  (see [22] for details). Based on the above observations and recalling that  $R_1^{\max}$  does not depend on  $F$ , we conclude that  $Q_2(\omega, F)$  increases with  $\omega$  while decreases with  $F$ . By consequence, the curve defined by the implicit equation  $Q_2(\omega, F) = 0$ , has non-negative derivative:

$$-\frac{\partial Q_2(\omega, F)}{\partial \omega} \Big/ \frac{\partial Q_2(\omega, F)}{\partial F} \geq 0.$$



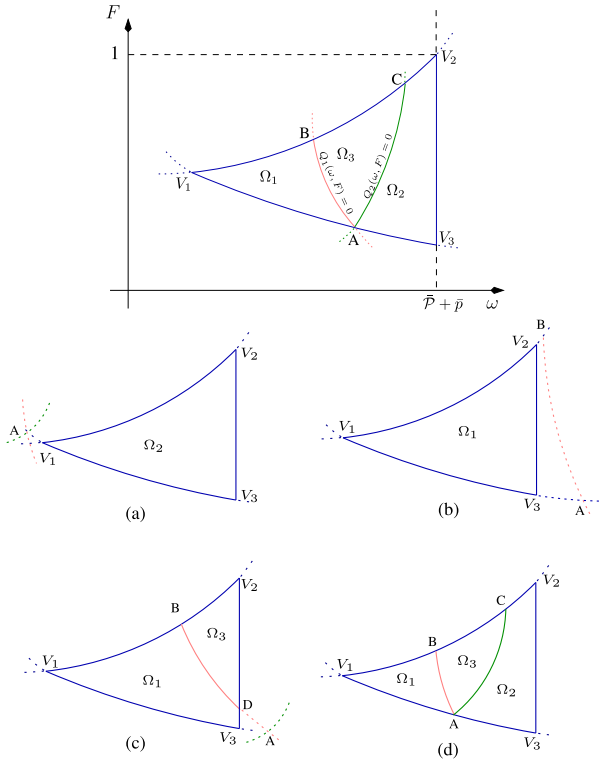


Fig. 3. (Top) A graphical representation of Region  $\Omega$  and its subregions  $\Omega_1$ ,  $\Omega_2$  and  $\Omega_3$ . (Bottom) A graphical representation of the subregions  $\Omega_1$ ,  $\Omega_2$ , and  $\Omega_3$  and of the cases when they exist.

Moreover, the curve  $Q_2(\omega, F) = 0$  intersects the edge  $V_1-V_3$  in  $A = \left(\omega_A, F_A = \frac{\bar{P}}{\omega_A}\right)$ , as it can be easily proven by observing that  $Q_2(\omega_A, F_A) = 0$ . The curve  $Q_2(\omega, F) = 0$  intersects the edge  $V_1-V_2$  in  $C = \left(\omega_C, F_C = \frac{\bar{P} + p^{\max} - \bar{p}}{p^{\max} - \omega_C}\right)$ .

Note that the curve  $Q_2(\omega, F) = 0$  never crosses the line  $\omega = \bar{P} + \bar{p}$ . Indeed, when  $\omega = \bar{P} + \bar{p}$ , the expression  $Q_2(\bar{P} + \bar{p}, F)$  does not depend on  $F$  any longer. As mentioned,  $R_1^{\max}$  decreases with  $\omega$  while  $\tilde{R}_2^{\min}$  increases with  $\omega$ ; thus,  $\Omega_2$  is located on the right of the curve  $Q_2(\omega, F) = 0$  (see Fig. 3(top)).

3) Finally, let  $\Omega_3 = \Omega \setminus (\Omega_1 \cup \Omega_2)$ . The maximum rate achieved in  $\Omega_3$  is denoted by  $R_{\Omega_3}$  and can be obtained by maximizing the rate  $R_1(g) = \tilde{R}_2(g)$  over  $g(\cdot)$ . To this end, in the region  $\Omega_3$ , we reformulate **P3** as follows:

$$\begin{aligned} \mathbf{P4:} \quad R_{\Omega_3} = & \max_{(\omega, F) \in \Omega_3} \left[ F \log(1 + \omega\beta_0) \right. \\ & \left. - F \min_{g(\cdot)} \int_0^\omega g(p) \log(1 + \beta_0 p) dp \right] \quad \text{s.t.} \quad (36) \\ & \int_0^\omega g(p) [\log(1 + \beta_0 p) + \log(1 + v p)] dp = C(\omega, F) \\ & \int_0^\omega p g(p) dp = \omega - \frac{\bar{P}}{F}; \quad \int_0^\omega g(p) dp = 1 \\ C(\omega, F) = & \log(1 + \beta_0 \omega) + \left(1 - \frac{1}{F}\right) \\ & \times \log\left(1 + v \frac{\bar{P} + \bar{p} - F\omega}{1 - F}\right) \quad (37) \end{aligned}$$

where we maximize with respect to  $\omega$ ,  $F$ , and  $g(\cdot)$ , and we impose  $R_1(g) = \tilde{R}_2(g)$ .

The maximum rate over  $\Omega$  is therefore given by  $R = \max\{R_{\Omega_1}, R_{\Omega_2}, R_{\Omega_3}\}$ . In the following, we state the conditions under which the three subregions  $\Omega_1$ ,  $\Omega_2$ , and  $\Omega_3$  exist.

#### D. Existence of Regions $\Omega_1$ , $\Omega_2$ , and $\Omega_3$

We first observe that, depending on the system parameters, the positions of the points  $A$  and  $B$  vary. Several cases are possible.

(a) Point  $A$  is located on the left of  $V_1$ , hence, outside  $\Omega$ . Since the curve  $Q_2(\omega, F) = 0$  intersects the edge  $V_1-V_2$  at most once, we conclude that in this case  $\Omega_2 = \Omega$ . This situation is depicted in (a) in Fig. 3(bottom) and arises when  $Q_2(V_1) \geq 0$ . By solving  $Q_2(V_1) \geq 0$  for  $\bar{P}$ , we obtain  $\bar{P} \leq \mathcal{P}_3 \triangleq \frac{p^{\max} - \bar{p}}{p^{\max} \beta_0} \left[ (1 + p^{\max} v)^{\frac{\bar{p}}{p^{\max} - \bar{p}}} - 1 \right]$ . Clearly,  $\Omega_1$  and  $\Omega_3$  do not exist in this case.

(b) Points  $A$  and  $B$  are located on the right of the points  $V_3$  and  $V_2$ , respectively, as depicted in (b) in Fig. 3(bottom). Since the curve  $Q_1(\omega, F) = 0$  intersects the edge  $V_2-V_3$  at most in a single point (as proved in Appendix E), in this case  $\Omega_1 = \Omega$ . The condition  $Q_1(V_2) \geq 0$  (i.e., for which  $B$  is on the right of  $V_2$ ), solved for  $\bar{P}$ , provides  $\bar{P} \geq \bar{p} \frac{v}{\beta_0} (1 + \bar{p}\beta_0) = \mathcal{P}_2$  while the condition  $Q_1(V_3) \geq 0$  (i.e., for which  $A$  is to the right of  $V_3$ ) is equivalent to  $\bar{p} \log(1 + v(\bar{P} + \bar{p})) \leq \bar{P} \log(1 + (\bar{P} + \bar{p})\beta_0)$  with solution  $\bar{P} \geq \mathcal{P}_4$ . Therefore, the above situation arises when  $\bar{P} \geq \max\{\mathcal{P}_2, \mathcal{P}_4\}$ .

(c) Point  $A$  is located on the right of  $V_3$  and  $B$  is on the left of  $V_2$ . Here, only regions  $\Omega_1$  and  $\Omega_3$  exist, as depicted in (c) in Fig. 3(bottom). This situation arises when  $Q_1(V_3) \geq 0$  and  $Q_1(V_2) \leq 0$ , i.e., for  $\mathcal{P}_4 \leq \bar{P} \leq \mathcal{P}_2$ . Furthermore, in this case the curve  $Q_1(\omega, F) = 0$  intersects the edge  $V_2-V_3$  in  $D$ .

(d) Point  $A$  lies on the edge connecting  $V_1$  and  $V_3$ . In this case, all regions  $\Omega_1$ ,  $\Omega_2$ , and  $\Omega_3$  exist, as depicted in (d) in Fig. 3(bottom). This situation happens when  $\mathcal{P}_3 \leq \bar{P} \leq \mathcal{P}_4$ .

#### E. Maximizing $R$ as the Average Source Transmit Power Varies

We consider the four cases reported in Fig. 3(bottom).

(a) For  $\bar{P} \leq \mathcal{P}_3$  (case depicted in (a) in Fig. 3(bottom)),  $R = R_{\Omega_2} = \max_{\Omega_2} R_1^{\max}$ . Since  $R_1^{\max}$  decreases with  $\omega$  and does not depend on  $F$ , the maximum is achieved in  $V_1$ . We then replace (35) and (28) in (20), set  $\omega$  and  $F$  to the coordinates of  $V_1$ , and find:

$$f^*(p) = \left(1 - \frac{\bar{p}}{p^{\max}}\right) \delta(p) + \frac{\bar{p}}{p^{\max}} \delta(p - p^{\max}).$$

Recalling that the source power is  $P(p) = \frac{\beta}{|h_1|^2} [\omega - p]^+$ , for  $p = 0$  we get  $P(p) = \frac{p^{\max} \bar{P}}{p^{\max} - \bar{p}}$ , while for  $p = p^{\max}$  we have  $P(p) = 0$ . The achieved rate becomes:

$$R = R_{\Omega_2} = \left(1 - \frac{\bar{p}}{p^{\max}}\right) \log\left(1 + \frac{p^{\max} \bar{P}}{(p^{\max} - \bar{p})\beta_0}\right).$$

(b) For  $\bar{P} \geq \max\{\mathcal{P}_4, \mathcal{P}_2\}$  (case depicted in (b) in Fig. 3(bottom)),  $R = R_{\Omega_1} = \max_{\Omega_1} \tilde{R}_2^{\max}$ . It can be easily

shown that  $\tilde{R}_2^{\max}$  increases with  $\omega$ , the values on the edge  $V_1-V_2$  monotonically increase with  $\omega$ , and the values on the edge  $V_1-V_3$  monotonically decrease with  $\omega$  (see [22] for details). We therefore conclude that the maximum of  $\tilde{R}_2^{\max}$  is located on the rightmost edge of  $\Omega_1$ , i.e., on the edge  $V_2-V_3$  where  $\omega = \bar{\mathcal{P}} + \bar{p}$ . Once we fix  $\omega$  to such value,  $\tilde{R}_2^{\max}|_{\omega=\bar{\mathcal{P}}+\bar{p}}$  increases with  $F$ . It follows that the rate is maximized in  $V_2$  and is given by  $R = R_{\Omega_1} = \log(1 + v\bar{p})$ . Moreover, by replacing (32) and (28) in (20) and by setting  $\omega = \bar{\mathcal{P}} + \bar{p}$  and  $F = 1$ , we obtain  $f^*(p) = \delta(p - \bar{p})$ . Since this is a single delta function, the source power can be computed for  $p = \bar{p}$  as:  $P(\bar{p}) = \frac{\beta}{|h_1|^2}[\omega - \bar{p}]^+ = \bar{P}$ .

(c) For  $\mathcal{P}_4 < \bar{\mathcal{P}} < \mathcal{P}_2$ , only subregions  $\Omega_1$  and  $\Omega_3$  exist, thus  $R = \max\{R_{\Omega_1}, R_{\Omega_3}\}$ . Let us first focus on  $\Omega_1$ . As observed before,  $R_{\Omega_1} = \max_{\Omega_1} \tilde{R}_2^{\max}$  where  $\tilde{R}_2^{\max}$  increases with  $\omega$ , thus  $\tilde{R}_2^{\max}$  is maximized on the edge  $B-D$  and on the segment  $D-V_3$  (where  $\omega = \bar{\mathcal{P}} + \bar{p}$ ). However, as mentioned for  $\omega = \bar{\mathcal{P}} + \bar{p}$ ,  $\tilde{R}_2^{\max}$  increases with  $F$ . It follows that the maximum must lie on the edge  $B-D$ .

As for the subregion  $\Omega_3$ , the maximum achievable rate is given by the solution of **P4**, which can be solved by using Theorem 2. We have that:

- if  $v \geq \beta_0$ , it can be shown that  $R_{\Omega_3}$  lies on the edge  $B-D$  (see [22] for details). Thus,  $R = R_{\Omega_1} = R_{\Omega_3}$  and  $R$  can be computed by solving  $R = \max_{Q_1(\omega, F)=0} R_1^{\min}$ , which is convex, hence, easy to be solved. Let  $(\omega^*, F^*)$  be the point where the rate is maximized, then the corresponding function  $f^*(p)$  is given by combining (28) with  $g(p) = \delta(p - \omega + \bar{\mathcal{P}}/F)$ , i.e.,

$$f^*(p) = F^* \delta(p - \omega^* + \bar{\mathcal{P}}/F^*) + (1 - F^*) \delta\left(p - \frac{\bar{\mathcal{P}} + \bar{p} - \omega^*}{1 - F^*} - \omega^*\right) \quad (38)$$

- otherwise, the problem can be solved numerically and the rate is maximized in  $V_2 = (\bar{\mathcal{P}} + \bar{p}, 1)$  [22]. The optimal distribution of the transmission power at the relay is then given by:

$$f^*(p) = \frac{p_2 - \bar{p}}{p_2} \delta(p) + \frac{\bar{p}}{p_2} \delta(p - p_2) \quad (39)$$

where  $p_2$  is the solution of the following constraint:

$$\frac{\log[(1 + \beta_0 p_2)(1 + v p_2)]}{p_2} = \frac{\log(1 + \beta_0 \omega) + (1 - \frac{1}{F}) \log\left(1 + v \frac{\bar{\mathcal{P}} + \bar{p} - F \omega}{1 - F}\right)}{\omega - \frac{\bar{\mathcal{P}}}{F}}. \quad (40)$$

(d) When  $\mathcal{P}_3 < \bar{\mathcal{P}} < \mathcal{P}_4$ , the situation is depicted in (d) in Fig. 3(bottom) where all three subregions exist. In subregion  $\Omega_1$ , following the same rationale as in case (c), we conclude that the rate  $R_{\Omega_1}$  lies on the edge  $B-A$ . In subregion  $\Omega_2$ , the rate is  $R_{\Omega_2} = \max_{\Omega_2} R_1^{\max}$ . Since  $R_1^{\max}$  does not depend on  $F$ , it decreases with  $\omega$ , and the implicit curve  $Q_2(\omega, F) = 0$  is monotonically increasing, we conclude that  $R_{\Omega_2}$  is obtained when operating in  $A$ . Hence,  $R_{\Omega_2} \leq R_{\Omega_1}$ . With regard to subregion  $\Omega_3$ , the maximum achievable rate is given by the

solution of **P4**, which can be solved by using Theorem 2. We have that:

- if  $v \geq \beta_0$ , as observed for case (c),  $R_{\Omega_3}$  lies on the edge  $B-A$ . Thus,  $R = R_{\Omega_1} = R_{\Omega_3}$  and  $R$  can be computed by solving  $R = \max_{Q_1(\omega, F)=0} R_1^{\min}$ ;
- else, similarly to the previous case, the problem can be solved numerically and the optimum is located in  $A = (\omega_A, F_A)$ . The optimal distribution of the transmission power at the relay is given by:

$$f^*(p) = F_A \delta(p) + (1 - F_A) \delta\left(p - \frac{\bar{p}}{1 - F_A}\right). \quad (41)$$

As done before, we use the obtained probability density function of the transmit power at the relay, to derive the optimal power allocation at the source node using (7). In Table II, we summarize our results highlighting the power allocation at both source and relay, the phases duration, and the data rate for the different cases analyzed above. Note that the expressions reported in the table hold only for  $0 \leq \bar{\mathcal{P}} < \mathcal{P}_0$ . By looking at the two top tables, we can make the following observations:

- for  $\bar{\mathcal{P}} \leq \mathcal{P}_3$ , the source transmits in phase B (i.e., the relay operates in HD-RX) while in phase A the relay operates in HD using its maximum power (HD-TX);
- for  $\bar{\mathcal{P}} \geq \max\{\mathcal{P}_2, \mathcal{P}_4\}$ , the relay operates in FD for the whole frame and both source and relay transmit at their average power;
- for  $\bar{\mathcal{P}} \in (\mathcal{P}_3, \max\{\mathcal{P}_2, \mathcal{P}_4\})$ ,  $v \geq \beta_0$ , the relay works in HD-TX in phase A and in FD in phase B;
- for  $\bar{\mathcal{P}} \in (\mathcal{P}_4, \max\{\mathcal{P}_2, \mathcal{P}_4\})$ ,  $v < \beta_0$ , the relay works in FD in phase A and in HD-RX in phase B;
- for  $\bar{\mathcal{P}} \in (\mathcal{P}_3, \mathcal{P}_4]$  and  $v < \beta_0$ , the relay works in HD-TX mode in phase A and in HD-RX in phase B; thus, this case corresponds to the traditional HD mode.

## VI. RESULTS

We compare the performance of our scheme to the ideal full duplex communication (referred to as “FD Ideal”) where the relay does not suffer from any self-interference. The performance of the “FD-Ideal” scheme is clearly unachievable when self-interference is present; it is therefore used as an upper bound for all the considered techniques. The corresponding rate is (see [12, eq.(38)])

$$R_{\text{FD-Ideal}} = \min \left\{ \log \left( 1 + \frac{\bar{P}|h_1|^2}{N_0} \right), \log \left( 1 + \frac{\bar{p}|h_2|^2}{N_0} \right) \right\}.$$

We then consider the full duplex scheme (referred to as “FD-IP”) where the source is aware of the instantaneous power (IP) at which the relay transmits. In FD-IP, the source always transmits with average power  $\bar{P}$  while the relay transmits with average power  $\bar{p}$ . We stress that, unlike FD-IP, our scheme only requires the knowledge at the source of the average power used at the relay. The expression of the rate

TABLE II

OPTIMAL POWER ALLOCATION AND RATE FOR  $0 \leq \bar{\mathcal{P}} < \mathcal{P}_0$ .  $t_A$  AND  $t_B = 1 - t_A$  ARE THE TIME FRACTIONS REPRESENTING THE PHASES DURATION. THE PHASES IN WHICH THE RELAY WORKS IN HD ARE SHADED

$v \geq \beta_0$		Phase A			Phase B		
		$t_A$	$P_A$	$p_A$	$t_B$	$P_B$	$p_B$
(a)	$\bar{\mathcal{P}} \in [0, \mathcal{P}_3]$	$\frac{\bar{p}}{p^{\max}}$	0	$p^{\max}$	$1 - \frac{\bar{p}}{p^{\max}}$	$\frac{\beta}{ h_1 ^2} \frac{p^{\max} \bar{p}}{p^{\max} - \bar{p}}$	0
(b)	$\bar{\mathcal{P}} \in [\max\{\mathcal{P}_2, \mathcal{P}_4\}, \infty)$	-	-	-	1	$\frac{\beta}{ h_1 ^2} \bar{\mathcal{P}}$	$\bar{p}$
(c), (d)	$\bar{\mathcal{P}} \in (\mathcal{P}_3, \max\{\mathcal{P}_2, \mathcal{P}_4\})$	$1 - F^*$	0	$\frac{\bar{\mathcal{P}} + \bar{p} - F^* \omega^*}{1 - F^*}$	$F^*$	$\frac{\beta}{ h_1 ^2} \frac{\bar{\mathcal{P}}}{F^*}$	$\omega^* - \frac{\bar{\mathcal{P}}}{F^*}$
$v < \beta_0$		Phase A			Phase B		
		$t_A$	$P_A$	$p_A$	$t_B$	$P_B$	$p_B$
(a)	$\bar{\mathcal{P}} \in [0, \mathcal{P}_3]$	$\frac{\bar{p}}{p^{\max}}$	0	$p^{\max}$	$1 - \frac{\bar{p}}{p^{\max}}$	$\frac{\beta}{ h_1 ^2} \frac{p^{\max} \bar{p}}{p^{\max} - \bar{p}}$	0
(b)	$\bar{\mathcal{P}} \in [\max\{\mathcal{P}_2, \mathcal{P}_4\}, \infty)$	1	$\frac{\beta}{ h_1 ^2} \bar{\mathcal{P}}$	$\bar{p}$	-	-	-
(c)	$\bar{\mathcal{P}} \in (\mathcal{P}_4, \max\{\mathcal{P}_2, \mathcal{P}_4\})$	$\frac{\bar{p}}{p_2}$	$\frac{\beta(\bar{\mathcal{P}} + \bar{p} - p_2)}{ h_1 ^2}$	$p_2$	$1 - \frac{\bar{p}}{p_2}$	$\frac{\beta(\bar{\mathcal{P}} + \bar{p})}{ h_1 ^2}$	0
(d)	$\bar{\mathcal{P}} \in (\mathcal{P}_3, \mathcal{P}_4]$	$1 - F_A$	0	$\frac{\bar{p}}{1 - F_A}$	$F_A$	$\frac{\beta \bar{\mathcal{P}}}{ h_1 ^2 F_A}$	0
		Rate $R$					
(a)	$\bar{\mathcal{P}} \in [0, \mathcal{P}_3]$	$(1 - \frac{\bar{p}}{p^{\max}}) \log \left( 1 + \frac{p^{\max} \bar{\mathcal{P}} \beta_0}{p^{\max} - \bar{p}} \right)$					
(b)	$\bar{\mathcal{P}} \in [\max\{\mathcal{P}_2, \mathcal{P}_4\}, \infty)$	$\log(1 + \bar{p}v)$					
(c), (d)	$\bar{\mathcal{P}} \in (\mathcal{P}_3, \max\{\mathcal{P}_2, \mathcal{P}_4\}); v \geq \beta_0$	$F^* \log \left( \frac{F^*(1 + \omega^* \beta_0)}{F^*(1 + \omega^* \beta_0) - \bar{\mathcal{P}} \beta_0} \right)$					
(c)	$\bar{\mathcal{P}} \in (\mathcal{P}_4, \max\{\mathcal{P}_2, \mathcal{P}_4\}); v < \beta_0$	$\log(1 + \beta_0(\bar{\mathcal{P}} + \bar{p})) - \frac{\bar{p}}{p_2} \log(1 + \beta_0 p_2)$					
(d)	$\bar{\mathcal{P}} \in (\mathcal{P}_3, \mathcal{P}_4]; v < \beta_0$	$F_A \log(1 + \beta_0 \omega_A)$					

achieved by FD-IP, also considered in [12], is<sup>2</sup>:

$$R_{\text{FD-IP}} = \min \left\{ \int_{-\infty}^{+\infty} \log \left( 1 + \frac{\bar{P} |h_1|^2}{N_0 + \beta x^2} \right) \frac{e^{-x^2/(2\bar{p})}}{\sqrt{2\pi\bar{p}}} dx, \right. \\ \left. \log \left( 1 + \frac{\bar{p} |h_2|^2}{N_0} \right) \right\}. \quad (42)$$

Furthermore, as done in [12], we compare our solution to the conventional half duplex scheme (named ‘‘HD’’), for which the rate is given by:

$$R_{\text{HD}} = \max_{\bar{p}/p^{\max} \leq t \leq 1} \min \left\{ (1-t) \log \left( 1 + \frac{|h_1|^2 \bar{P}}{(1-t)N_0} \right), \right. \\ \left. t \log \left( 1 + \frac{\bar{p} |h_2|^2}{tN_0} \right) \right\} \quad (43)$$

where the relay always operates in half duplex and its transmit power is limited to  $p^{\max}$ . This scheme implies that the communication is organized in two phases of relative duration  $t$  and  $1 - t$ , respectively.

Finally, we consider a scheme similar to the one proposed in [12] but without knowledge of the instantaneous transmitted symbols. Specifically, we compare with a hybrid communication scheme named FD-HD where the source has only knowledge of the instantaneous power used by the relay and the relay leverages on FD-IP or on HD, depending on which operational mode provides the highest rate. FD-HD is organized in the following three phases: (A) the source transmits at power  $P_A$  for a time fraction  $t_A$  while the relay is silent; (B) the source is silent and the relay transmits at power  $p_B$  for a time fraction  $t_B$ ; (C) the relay operates in FD, source and relay transmit at power  $P_C$  and  $p_C$ , respectively,

for a time fraction  $t_C$ . The achieved rate is given by:

$$R_{\text{FD-HD}} = \max_{\substack{t_A, t_B, t_C \\ P_A, P_C \\ p_B, p_C}} \min \left\{ t_A \log \left( 1 + \frac{P_A |h_1|^2}{N_0} \right) \right. \\ \left. + t_C \int_{-\infty}^{+\infty} \log \left( 1 + \frac{P_C |h_1|^2}{N_0 + \beta x^2} \right) \frac{e^{-x^2/(2p_C)}}{\sqrt{2\pi p_C}} dx, \right. \\ \left. t_B \log \left( 1 + \frac{p_B |h_2|^2}{N_0} \right) + t_C \log \left( 1 + \frac{p_C |h_2|^2}{N_0} \right) \right\} \quad (44)$$

where the first argument of the min operator represents the rate achieved on the source-relay link, the second one represents the rate achieved on the relay-destination link, and the following constraints must hold:  $t_A + t_B + t_C = 1$ ,  $t_A P_A + t_C P_C = \bar{P}$ ,  $t_B p_B + t_C p_C = \bar{p}$ , and  $p_B, p_C \leq p^{\max}$ .

In order to evaluate the performance of our solution against the above schemes, we consider a scenario similar to that employed in [12] where the source-relay and relay-destination distances are both set to  $d = 500$  m, the signal carrier frequency is  $f_c = 2.4$  GHz and the path loss is given by  $|h_1|^2 = |h_2|^2 = \left( \frac{c}{4\pi f_c} \right)^2 d^{-\alpha}$ , with  $\alpha = 3$ . Considering an additive noise with power spectral density  $-204$  dBW/Hz and a bandwidth  $B = 200$  kHz, the noise power at both relay and destination receivers is about  $N_0 = -151$  dBW. Note that, for this setting, we have  $v = |h_1|^2/N_0 \approx 30$  dB.

Fig. 4(left) compares the rate of our optimal power allocation scheme, labeled ‘‘OP’’, against the performance of FD-Ideal, FD-IP, FD-HD and HD, for  $\bar{p} = -10$  dBW,  $p^{\max} = -7$  dBW and  $\beta = -135$  dB. Since  $\beta_0 = \beta/N_0 \approx 16$  dB, the results we derived for  $v > \beta_0$  apply. Let  $P_i = p_i \frac{\beta}{|h_1|^2}$ , for  $i = 0, \dots, 4$ . For the parameters used in this example, the value of the power thresholds are:  $P_0 = -24$  dBW,  $P_1 = -14.23$  dBW,  $P_2 = -3.04$  dBW,  $P_3 = -9.92$  dBW, and  $P_4 = -20.56$  dBW. The thresholds  $P_3$  and  $P_4$  are meaningful

<sup>2</sup>We further note that the symbols are Gaussian distributed, thus the probability that they transmit a symbol  $x = 0$  is 0. It follows that the system always works in FD mode.

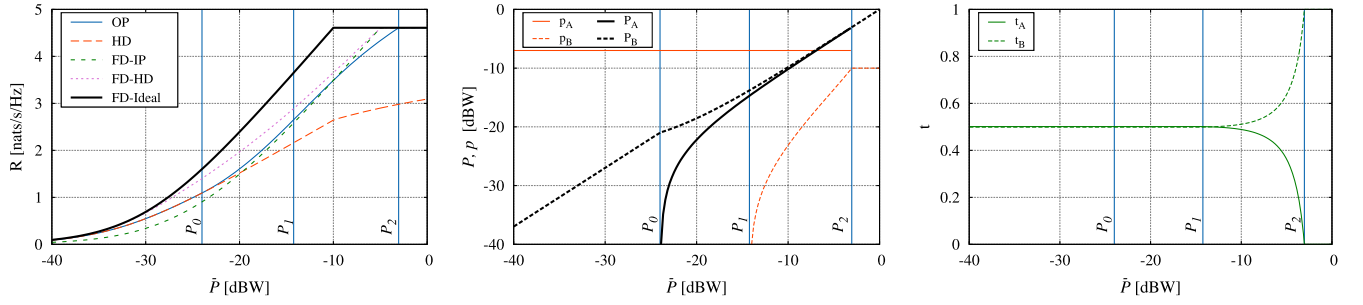


Fig. 4. Performance for  $\bar{p} = -10$  dBW,  $p^{\max} = -7$  dBW and  $\beta = -135$  dB: (left) Achieved rate vs.  $\bar{P}$ ; (middle) Optimal source and relay transmit power for phase A (solid lines) and phase B (dashed lines); (right) Phase durations  $t_A$  (solid line) and  $t_B$  (dashed line).

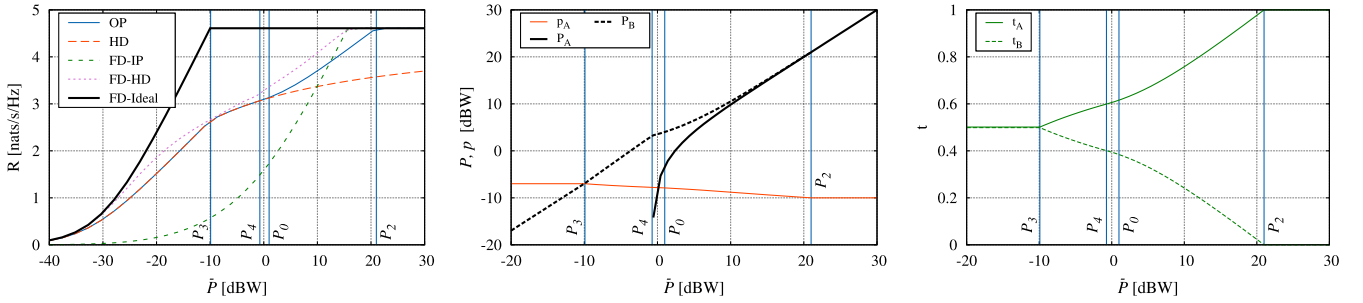


Fig. 5. Performance for  $\bar{p} = -10$  dBW,  $p^{\max} = -7$  dBW and  $\beta = -110$  dB: (left) Achieved rate vs.  $\bar{P}$ ; (middle) Optimal source and relay transmit power for phase A (solid lines) and phase B (dashed lines); (right) Phase durations  $t_A$  (solid line) and  $t_B$  (dashed line).

only if lower than  $P_0$  (see Sec. V), thus they are not shown in the figure. The achieved rates are depicted as functions of the average transmit power at the source,  $\bar{P}$ . For  $\bar{P} \geq P_0$ , the results obtained in Sec. IV hold. Accordingly, the plot highlights three operational regions corresponding to  $P_0 \leq \bar{P} \leq P_1$ ,  $P_1 < \bar{P} \leq P_2$ , and  $\bar{P} > P_2$ , respectively. Instead, for  $\bar{P} < P_0$  (see Sec. V), we have a single operational region only, since  $P_3 > P_0$  and  $P_4 > P_0$ . As expected, the performance of all communication strategies is upper-bounded by FD-Ideal, since the latter assumes no self-interference at the relay. Also, FD-HD outperforms both FD-IP and HD since it assumes perfect knowledge at the source about the instantaneous relay transmit power (as FD-IP) and can work in either FD or HD mode, depending on the system parameters. The proposed OP technique always outperforms HD and achieves higher rates than FD-IP for  $\bar{P} < -10$  dBW. Furthermore, OP gets very close to FD-HD, especially for  $\bar{P} > P_1$ .

Such performance of the OP scheme is achieved for the source and relay transmit power levels and for the phase durations depicted in Figs. 4(middle) and 4(right), respectively. Interestingly, for  $\bar{P} < P_1$ , the time durations of the two communication phases remain constant. With regard to the transmit power, for  $\bar{P} < P_0$ , the source transmits in phase B and is silent in phase A while the relay only transmits in phase A at its maximum power. For  $P_0 \leq \bar{P} < P_1$ , the source always transmits (even if at different power levels), while the relay only receives in phase B and transmits at its maximum power in phase A. For  $P_1 \leq \bar{P} < P_2$ , both source and relay transmit but the duration of the two phases varies, with  $t_A \rightarrow 0$  as  $\bar{P} \rightarrow P_2$ . Finally, for  $\bar{P} \geq P_2$ , both source and relay transmit at their average power level.

Fig. 5(left) refers to the same scenario as that considered in Fig. 4(left), but with the self-interference attenuation factor,  $\beta$ , set to  $-110$  dB. In this case,  $\beta_0 = \beta/N_0 \approx 41$  dB and the results obtained for  $v < \beta_0$  apply. Moreover, we have:  $P_0 = 1$  dBW,  $P_2 = 21$  dBW,  $P_3 = -9.9$  dBW, and  $P_4 = -0.7$  dBW, while the threshold  $P_1$  is not meaningful (hence, it is not shown). The figure highlights two operational regions for  $\bar{P} \geq P_0$  (namely,  $P_0 \leq \bar{P} \leq P_2$  and  $\bar{P} \geq P_2$ ), and three operational regions for  $\bar{P} < P_0$  (i.e.,  $\bar{P} < P_3$ ,  $P_3 \leq \bar{P} \leq P_4$  and  $P_4 < \bar{P} < P_0$ ). In this case too, OP outperforms FD-IP (except for high values of  $\bar{P}$ ) and performs very close to FD-HD. By looking at Fig. 5(middle), which depicts the corresponding power levels used at source and relay, we note that in phase B the relay is always silent. In phase A, instead, the relay transmits at its maximum power (namely,  $-7$  dBW) when  $\bar{P} \leq P_3$ , and it slowly decreases its power to  $\bar{p}$  as  $\bar{P}$  approaches  $P_2$ . With regard to the source, in phase B it always transmits for  $\bar{P} < P_2$ , although at different power levels depending on  $\bar{P}$ . On the contrary, in phase A it is silent for  $\bar{P} < P_4$ , and it always transmits for larger values of  $\bar{P}$ . These results match the values of the phase durations depicted in Fig. 5(right): now, the region where the phase durations are constant is limited to  $\bar{P} < P_3$ , while, as  $\bar{P}$  approaches  $P_2$ ,  $t_A \rightarrow 1$  and  $t_B \rightarrow 0$ .

Fig. 6(left) highlights the impact of self-interference on the network performance by showing the rate versus  $\bar{P}$ , achieved by OP and its counterpart FD-HD, as  $\beta$  varies. For completeness, the results for FD-Ideal and HD (which do not depend on  $\beta$ ) are shown too. For  $\beta = -120$  dB (i.e.,  $v < \beta_0$ ), the system is affected by a substantial self-interference at the relay, and OP performs as HD for low-medium values of  $\bar{P}$ .



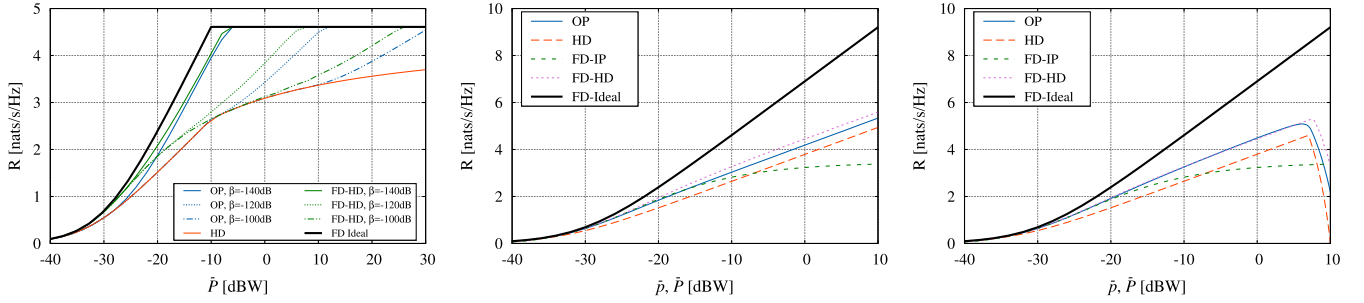


Fig. 6. (Left) Achieved rate vs.  $\bar{P}$ , for  $\bar{p} = -10$  dBW,  $p^{\max} = -7$  dBW, and different values of  $\beta$ ; (middle) Achieved rate vs.  $\bar{P} = \bar{p}$ , for  $p^{\max} = \bar{p} + 3$  dB and  $\beta = -130$  dB; (right) Achieved rate vs.  $\bar{P} = \bar{p}$ , for  $p^{\max} = 10$  dBW and  $\beta = -130$  dB.

As  $\beta$  (i.e., the self-interference) decreases, the OP performance becomes closer to that of FD-HD and FD-Ideal; in particular, for  $\beta = -140$  dB, the gap between OP and FD-HD reduces to about 1 dB.

In Fig. 6(middle), we study a different scenario where  $\beta$  is fixed to  $-130$  dB,  $\bar{p}$  and  $\bar{P}$  vary, and  $p^{\max} = \bar{p} + 3$  dB. Since now  $\bar{P}$ ,  $\bar{p}$  and  $p^{\max}$  can all grow very large, the gap between FD-Ideal and all other schemes becomes much more evident. However, OP closely matches FD-HD and significantly outperforms HD. Interestingly, FD-IP provides a lower rate than HD as the transmit power at source and relay increases. This is because FD-IP cannot exploit the HD mode; thus, when  $\bar{p}$  is large and the impact of self-interference becomes severe, there is no match with the other schemes.

Finally, Fig. 6(right) addresses a similar scenario to the one above, but  $p^{\max}$  is now fixed to 10 dBW. We observe that, as  $\bar{p}$  grows, the rate provided by all schemes increases. However, when  $\bar{p}$  approaches  $p^{\max}$ , the relay is constrained to transmit, i.e., to work in FD, for an increasingly longer time. For  $\bar{p} = p^{\max}$ , the relay always transmits at a power level equal to  $\bar{p} = p^{\max}$ . Also, the rate provided by the HD scheme drops to 0 while FD-IP and FD-HD provide the same performance; indeed, the latter cannot exploit anymore the advantages of HD. For the same reason, the OP scheme experiences a rate decrease. These results clearly suggest that significantly better performance can be achieved when  $\bar{p}$  is not too close to  $p^{\max}$ .

## VII. EXTENSION TO FINITE $P^{\max}$

The analysis performed in Secs. IV and V as well as the numerical results reported in Sec. VI have been obtained by assuming  $P^{\max}$  to be very large. By removing this assumption, the transmission power at the source can be written as in 6. We recall that, for simplicity, we defined  $\mathcal{P}^{\max} = \frac{|h_1|^2}{\beta} P^{\max}$  so that  $P(p)$  can be more conveniently written as  $P(p) = \frac{\beta}{|h_1|^2} \mathcal{P}(p)$  with  $\mathcal{P}(p) = \min\{[\omega - p]^+, \mathcal{P}^{\max}\}$ .

The following cases can occur:

- $\mathcal{P}^{\max} > \omega$ , then  $\mathcal{P}(p) = [\omega - p]^+$ . This leads to a situation similar to that considered in Secs. IV and V. Indeed,
  - in Sec. IV, by imposing  $\omega \geq p^{\max}$  in constraints (c), (d), and (e) of problem **P1**, we obtained  $\omega = \bar{P} + \bar{p}$ . It follows that  $\bar{P}$  should lie in the range  $[p^{\max} - \bar{p}, \mathcal{P}^{\max} - \bar{p}]$  where the results reported in Table I hold;

- in Sec. V, we considered the case  $\omega < p^{\max}$ . Since  $\mathcal{P}^{\max} > \omega$ , we obtain  $\omega < \min\{p^{\max}, \mathcal{P}^{\max}\}$ . If  $\mathcal{P}^{\max} > p^{\max}$  the results shown in Table II hold, otherwise they need to be recomputed by simply considering  $\omega$  ranging in  $[0, \mathcal{P}^{\max})$ .

- $\mathcal{P}^{\max} \leq \omega$ , which is a more challenging scenario to analyse. Indeed, in such a situation function  $\mathcal{P}(p)$ , with  $p \in [0, p^{\max}]$ , takes values in up to three linear regions, depending on the value of  $p^{\max}$ . Specifically,
  - if  $p^{\max} < \omega - \mathcal{P}^{\max}$ , we have  $\mathcal{P}(p) = \mathcal{P}^{\max}$ . Then the integral in (3) holds only if  $\bar{P} = \mathcal{P}^{\max}$ . This corresponds to the case where the source always transmits at its maximum power, regardless what the relay does;
  - if  $\omega - \mathcal{P}^{\max} \leq p^{\max} < \omega$ ,  $\mathcal{P}(p)$  takes values in two linear regions, i.e.,  $\mathcal{P}(p) = \mathcal{P}^{\max}$  if  $p \in [0, \omega - \mathcal{P}^{\max})$ , and  $\mathcal{P}(p) = \omega - p$  if  $p \in [\omega - \mathcal{P}^{\max}, p^{\max})$ . In order to maximize the rate  $R$  over the distribution  $f(p)$ , we then need to split it in two parts as done in Sec. V and the same analysis therein applies;
  - if  $p^{\max} \geq \omega$ ,  $\mathcal{P}(p)$  is composed of three linear regions, i.e.,  $\mathcal{P}(p) = \mathcal{P}^{\max}$  if  $p \in [0, \omega - \mathcal{P}^{\max})$ ,  $\mathcal{P}(p) = \omega - p$  if  $p \in [\omega - \mathcal{P}^{\max}, \omega)$ , and  $\mathcal{P}(p) = 0$  otherwise. In this case, for any given  $\omega$ , the rate maximization can be solved by splitting  $f(p)$  in three distributions having support in  $[0, \omega - \mathcal{P}^{\max})$ ,  $[\omega - \mathcal{P}^{\max}, \omega)$ , and  $[\omega, p^{\max}]$ , and having masses  $F_1(\omega)$ ,  $F_2(\omega)$ , and  $1 - F_1(\omega) - F_2(\omega)$ , respectively. The maximization can be performed following a procedure similar to Sec. V, although in this case, we need to consider a three-dimensional (instead of a bi-dimensional) region  $\Omega$ , with coordinates  $(\omega, F_1, F_2)$ . Such maximization is quite cumbersome if performed analytically.

## VIII. CONCLUSIONS

We investigated the maximum achievable rate in dual-hop decode-and-forward networks where the relay can operate in full-duplex mode. Unlike existing work, in our scenario the source is only aware of the probability density function of the transmit power at the relay; under this assumption, we derived the allocation of the transmit power at the source and relay that maximize the data rate. Such probability density function turned out to be discrete and composed of either one or two delta functions. This finding allowed us to identify the optimal network communication strategy, which, in general, is given

by a two-phase scheme where the relay operates in HD or FD in each phase. Our numerical results highlight the advantage of being able to gauge full-duplex and half-duplex at the relay, depending on the channel gains and the amount of self-interference affecting the system. They also underline the excellent performance of the proposed scheme, even when compared to strategies that assume the source to be aware of the instantaneous transmit power at the relay.

#### APPENDIX A

We can solve **P0** by writing Lagrange's equation and leveraging the well-known Karush-Kuhn-Tucker (KKT) conditions. We define the Lagrangian as:

$$\mathcal{L}(P) = f(p) \log \left( 1 + \frac{|h_1|^2 P(p)}{N_0 + \beta p} \right) - \lambda (f(p)P(p) - \bar{P}) - \mu_1(p)(P(p) - P^{\max}) + \mu_2(p)P(p) \quad (45)$$

where  $\mu_1(p), \mu_2(p) \geq 0$  and  $\lambda$  are the KKT multipliers. Writing the KKT conditions, we obtain  $\frac{f(p)|h_1|^2}{N_0 + \beta p + P(p)|h_1|^2} - \lambda f(p) - \mu_1(p) + \mu_2(p) = 0$ ,  $\mu_1(p)(P(p) - P^{\max}) = 0$ , and  $\mu_2(p)P(p) = 0$ , along with (a) and (b) that must still hold. It can be easily verified that the above system is satisfied when  $\mu_1(p) = \mu_2(p) = 0$ , for which the first KKT condition reduces to  $f(p) \left[ \frac{|h_1|^2}{N_0 + \beta p + P(p)|h_1|^2} - \lambda \right] = 0$ . Solving for  $P(p)$  we get:  $P(p) = \frac{\beta}{|h_1|^2} \min \{ [\omega - p]^+, P^{\max} \}$  where we defined  $P^{\max} \triangleq P^{\max} \frac{|h_1|^2}{\beta}$ , and  $\omega = \frac{|h_1|^2}{\beta \lambda} - \frac{N_0}{\beta}$ , which must satisfy (a).

#### APPENDIX B

The upper bound is immediately obtained by applying Jensen inequality and it clearly holds with equality when  $f(p) = \delta(p - m)$ . With regard to the lower bound, being  $\phi(p)$  concave in  $p \in [a, b]$ , we can write  $\phi(p) \geq \frac{\phi(b) - \phi(a)}{b-a}(p - a) + \phi(a)$ . Therefore,  $\int_a^b f(p)\phi(p) dp \geq \frac{b-m}{b-a}\phi(a) + \left(1 - \frac{b-m}{b-a}\right)\phi(b)$ . For  $f(p) = \frac{b-m}{b-a}\delta(p - a) + \left(1 - \frac{b-m}{b-a}\right)\delta(p - b)$ , the lower bound holds with equality.

#### APPENDIX C

The conditions  $\omega \in [0, P^{\max})$ ,  $F \in [0, 1]$ ,  $0 \leq G \leq \bar{P}$ , (24), and (25) can be rewritten in terms of  $F$  and  $\omega$  as follows: (a)  $F \leq \frac{\bar{P} + \bar{P}}{\omega}$ ; (b)  $F \leq \frac{P^{\max} - \bar{P} - \bar{P}}{P^{\max} - \omega}$ ; (c)  $F \geq \frac{\bar{P}}{\omega}$ ; (d)  $\omega < \bar{P} + \bar{p}$ ; (e)  $0 \leq F \leq 1$ ; (f)  $0 \leq \omega < P^{\max}$ . Note that (d) implies  $\frac{\bar{P} + \bar{p}}{\omega} > 1$ . Since  $F \leq 1$ , condition (a) is always verified, hence it is redundant. Similarly, since  $\bar{P}$  and  $\omega$  are both positive, we have  $\frac{\bar{P}}{\omega} \geq 0$ ; thus the left inequality in (e) is redundant. Also, it is easy to check that  $\frac{P^{\max} - \bar{P} - \bar{P}}{P^{\max} - \omega} \leq 1$  implies  $\omega \leq \bar{P} - \bar{P}$ , which is more restrictive than (d); thus, the right inequality in (e) is redundant. In conclusion, the remaining constraints on  $F$  can be summarized as  $\frac{\bar{P}}{\omega} \leq F \leq \frac{P^{\max} - \bar{P} - \bar{P}}{P^{\max} - \omega}$ . Clearly, solutions for  $F$  exist if and only if  $\frac{\bar{P}}{\omega} \leq \frac{P^{\max} - \bar{P} - \bar{P}}{P^{\max} - \omega}$ , i.e., if and only if  $\omega \geq \frac{P^{\max} \bar{P}}{P^{\max} - \bar{P}}$ . Since term  $\frac{P^{\max} \bar{P}}{P^{\max} - \bar{P}}$  is positive, the remaining conditions on  $\omega$  can be summarized as  $\frac{P^{\max} \bar{P}}{P^{\max} - \bar{P}} \leq \omega < \min\{P^{\max}, \bar{P} + \bar{p}\}$ . Hence, a solution for  $\omega$  exists if and

only if  $\frac{P^{\max} \bar{P}}{P^{\max} - \bar{P}} < P^{\max}$  and  $\frac{P^{\max} \bar{P}}{P^{\max} - \bar{P}} < \bar{P} + \bar{p}$ ; such conditions are satisfied when  $\bar{P} < P^{\max} - \bar{p} = \mathcal{P}_0$ . In conclusion, under the condition  $\bar{P} < \mathcal{P}_0$ , a solution for the above inequalities exists and it is represented by the region  $\Omega$  in (26).

#### APPENDIX D

The problem in (14) can be solved by using the Euler-Lagrange formula. We define the Lagrangian  $L(p, f(p)) = f(p)\phi(p) + \lambda_1 f(p)\psi(p) + \lambda_2 pf(p) + \lambda_3 f(p) - \mu(p)f(p)$  where the first term represents the functional to be minimized. The second, third and fourth terms represent the constraints (a), (b), and (c) with associated Lagrange multipliers  $\lambda_1$ ,  $\lambda_2$  and  $\lambda_3$ , respectively. Note that (d) can be rewritten as  $-f(p) \leq 0$  and it requires a Lagrange multiplier for every  $p \in [a, b]$ . This can be done by introducing the multiplier  $\mu(p) \geq 0$ .

Next, we apply the Euler-Lagrange formula and we write the KKT conditions associated with the problem. Specifically, we get  $\frac{\partial L}{\partial f} = 0 \Rightarrow \mu(p) = \phi(p) + \lambda_1 \psi(p) + \lambda_2 p + \lambda_3$ , subject to the conditions (a), (b), (c), (d),  $\mu(p) \geq 0$ , and  $\mu(p)f(p) = 0$ .

Now the key observation is that  $\mu(p) = \phi(p) + \lambda_1 \psi(p) + \lambda_2 p + \lambda_3$  identifies a family of continuous functions driven by the parameters  $\lambda_1$ ,  $\lambda_2$  and  $\lambda_3$ . Such parameters need to be properly chosen in order to have  $\mu(p) \geq 0, \forall p \in [a, b]$ . If  $\mu(p)$  is strictly positive in  $[a, b]$  (i.e.,  $\mu(p) > 0, \forall p \in [a, b]$ ), then the condition  $\mu(p)f(p) = 0$  implies  $f(p) = 0, \forall p \in [a, b]$ , which is not a valid solution. Moreover,  $\phi(p)$  and  $\psi(p)$  are not constant functions, therefore it is not possible to find values of the Lagrange multipliers such that  $\mu(p) = 0$ , in a subset of  $[a, b]$  having non-zero measure. The only option is to allow  $\mu(p) > 0$  for all  $p \in [a, b]$ , except for a discrete set of points  $p_i \in [a, b]$  for which  $\mu(p_i) = 0$ . This observation hints that the solution of the problem must be found in the set of discrete distributions. In practice, every solution  $p_i$  of  $\mu(p) = 0$  is associated with a mass of probability,  $\pi_i$ , located at  $p_i$ .

The number of solutions of  $\mu(p) = 0$  can vary depending on the values of  $\lambda_1$ ,  $\lambda_2$ ,  $\lambda_3$ ,  $\gamma_1$ , and  $\gamma_2$ . In general, such a number can be computed by analyzing the first derivative of  $\mu(p)$ :  $\mu'(p) = \frac{k_1 p^2 + k_2 p + k_3}{(1 + \gamma_1 p)(1 + \gamma_2 p)}$  where  $k_1, k_2, k_3$  depend on  $\lambda_1, \lambda_2, \lambda_3, \gamma_1, \gamma_2$ . The numerator of  $\mu'(p)$  is a polynomial in  $p$  of degree 2 and thus has up to two solutions for  $p$  in  $[a, b]$ , which correspond to local minima or maxima of  $\mu(p)$ . Let  $f^*(p)$  be the minimizer of (14). Then several cases are possible:

1)  $\mu(p)$  has a single solution  $p_1 \in [a, b]$ , which does not correspond to local minima or maxima. Then  $p_1 = a$  or  $p_1 = b$ . This implies  $f^*(p) = \pi_1 \delta(p - a)$  (or,  $f^*(p) = \pi_1 \delta(p - b)$ ) which, however has only one degree of freedom (i.e., the value of  $\pi_1$ ) and thus, in general, cannot satisfy constraints (a), (b), and (c) of (14) all together;

2)  $\mu(p)$  has a single solution  $p_1 \in [a, b]$ , which corresponds to a local minimum. Thus  $f^*(p) = \pi_1 \delta(p - p_1)$ . However, this solution is not feasible since it has only two degrees of freedom (i.e.,  $p_1$  and  $\pi_1$ ) and therefore, in general, cannot satisfy the three constraints (a), (b), and (c) of (14) at the same time;

3)  $\mu(p)$  has two solutions  $p_1, p_2 \in [a, b]$  none of which corresponds to a local minimum. Thus  $p_1 = a$  and  $p_2 = b$ , and  $f^*(p) = \pi_1\delta(p - a) + \pi_2\delta(p - b)$ . Again, in general, this solution is not feasible since it has only two degrees of freedom ( $\pi_1$  and  $\pi_2$ ) and therefore cannot meet (a), (b), and (c) at the same time;

4)  $\mu(p)$  has two solutions  $p_1, p_2 \in [a, b]$  one of which is a local minimum. Then two cases are possible, i.e.,  $\{p_1 = a, p_2 > a\}$  or  $\{p_1 < b, p_2 = b\}$  and the minimizer  $f^*(p)$  takes the expression  $f^*(p) = \pi_1\delta(p - a) + \pi_2\delta(p - p_2)$  or  $f^*(p) = \pi_1\delta(p - p_1) + \pi_2\delta(p - b)$ . This solution is feasible since it has three degrees of freedom represented by  $\{\pi_1, \pi_2, p_1\}$  or  $\{\pi_1, \pi_2, p_2\}$  that can be determined by imposing the constraints (a), (b), and (c). The constants  $\gamma_1$ , and  $\gamma_2$  determine which of the two expressions in (15) is the minimizer. This is shown below.

Since  $\mu(p)$  cannot have more than two distinct solutions in  $[a, b]$  (indeed,  $\mu'(p)$  has at most two solutions), we conclude that the minimizer of (14) is given by (15).

*Selecting the minimizer expression.* The minimizer can assume one of the two possible expressions in (15). Here we show that the choice of the minimizer depends on the parameters  $\gamma_1$  and  $\gamma_2$ . To do so, we first observe that the family of distributions  $f^*(p, x, y) = \pi(x, y)\delta(p - x) + [1 - \pi(x, y)]\delta(p - y)$ , where  $\pi(x, y) = \frac{y-m}{y-x} > 0$  with  $m \leq y \leq b$  and  $a \leq x \leq m$ , encompasses both expressions in (15). Specifically, the expressions reported in (15) are given by  $f^*(p, a, p_2)$  and  $f^*(p, p_1, b)$ , respectively.

For such a family of distributions, constraint (a) in (14) can be rewritten as  $F(x, y) = \int_a^b f^*(p, x, y)\psi(p)dp = \pi(x, y)\psi(x) + [1 - \pi(x, y)]\psi(y) = c$ . Similarly, the cost function,  $\int_a^b f(p)\phi(p)dp$ , can be written as  $G(x, y) = \pi(x, y)\phi(x) + [1 - \pi(x, y)]\phi(y)$ . Note that, since  $\psi(p) = \phi(p) + \eta(p)$ , we have  $F(x, y) = G(x, y) + H(x, y)$  where  $H(x, y) = \pi(x, y)\eta(x) + [1 - \pi(x, y)]\eta(y)$ . In the following, for the sake of notation simplicity, we drop the argument of the functions when not needed. We now make the following observations:

1)  $F$  and  $G$  are increasing functions of  $x$  and decreasing functions of  $y$  [22].

2) the equation  $F(x, y) = c$  is the implicit definition of  $y_c(x)$ ,  $a \leq x \leq p_1$  and  $p_2 \leq y \leq b$  with derivative defined as  $y'_c(x) = \frac{dy_c(x)}{dx} = -\frac{F_x}{F_y}$  where we defined  $F_x = \frac{\partial F}{\partial x}$  and  $F_y = \frac{\partial F}{\partial y}$ . By the above arguments on the partial derivatives of  $F$ , we conclude that  $y'_c(x) > 0$ . Similarly, the function  $G(x, y) = t$  is the implicit definition of  $y_t(x)$  whose derivative  $y'_t(x)$  is positive.

3) Given the constant  $c$ , a value for  $t$  exists such that  $y_c(x)$  and  $y_t(x)$  have a common solution  $(x^*, y^*)$ . E.g., if  $t = G(a, p_2)$ , the two curves share the point  $(a, y_c(a))$ . Now consider a value of  $t$  such that the curves  $y_c(x)$  and  $y_t(x)$  intersect at point  $P = (x^*, y^*)$ , with  $P \neq (a, p_2)$ ,  $P \neq (p_1, b)$ . If  $y'_c(x) > y'_t(x)$  at  $P$ , then  $t$  is not the global minimum of the cost function in (14). Indeed, it exists  $\epsilon > 0$  such that the curve  $y_{t-\epsilon}(x)$  intersects  $y_c(x)$  at some point  $P' = (x^* + \Delta_x, y^* + \Delta_y)$  where the cost function  $G(x^* + \Delta_x, y^* + \Delta_y) = t - \epsilon$  is clearly lower than at  $P$ . Since this is true for any point

$P = (x^*, y^*)$ , we conclude that the minimizer is  $f^*(p, p_1, b)$  and that the minimum is  $G(p_1, b)$ . By applying similar arguments, if  $y'_c(x) < y'_t(x)$  at  $P$  the minimizer is  $f^*(p, a, p_2)$  and the minimum is  $G(a, p_2)$ .

To compare the derivatives of  $y'_c(x)$  and  $y'_t(x)$ , we use the definitions of  $F$ ,  $G$ , and  $H$  and write:  $y'_c(x) = -\frac{F_x}{F_y} = -\frac{G_x + H_x}{G_y + H_y}$  and  $y'_t(x) = -\frac{G_x}{G_y}$  where  $G_x, H_x, G_y, H_y$  are the partial derivatives of  $G$  and  $H$  w.r.t.  $x$  and  $y$ , respectively. By considering  $y'_c(x) \geq y'_t(x)$ , we obtain  $-\frac{G_x + H_x}{G_y + H_y} \geq -\frac{G_x}{G_y} \Rightarrow -\frac{G_x}{G_y} \leq -\frac{H_x}{H_y}$ . We also observe that:  $\frac{\partial \pi}{\partial x} = \pi_x = \frac{\pi}{y-x}$  and  $\frac{\partial \pi}{\partial y} = \pi_y = \frac{1-\pi}{y-x}$ . We can easily derive the expressions of  $G_x, G_y, H_x$  and  $H_y$ . Now observe that  $\phi(p) = \log(1 + \gamma_1 p)$  and  $\eta(p) = \log(1 + \gamma_2 p)$  are the same function (i.e.,  $\log(1 + \gamma p)$ ), the former evaluated in  $\gamma = \gamma_1$  and the latter in  $\gamma = \gamma_2$ . Therefore, since  $G$  depends on  $\phi(p)$  and  $H$  depends on  $\eta(p)$ , we can write  $-\frac{G_x}{G_y} = \zeta(\gamma_1)$  and  $-\frac{H_x}{H_y} = \zeta(\gamma_2)$ . It is easy to show that  $\zeta(\gamma)$  increases with  $\gamma$ ; indeed, by imposing  $\zeta'(\gamma) \geq 0$ , after some algebra and after simplifying positive factors, we obtain:  $\log\left(\frac{1+\gamma y}{1+\gamma x}\right)(2+\gamma y+\gamma x) \geq 2\gamma(y-x)$ . The right hand side (r.h.s.) of the previous inequality is positive and linear with  $\gamma$ ,  $\gamma \geq 0$ . The left hand side (l.h.s.) is positive, convex and tangent to the r.h.s. at  $\gamma = 0$ . Therefore, the above inequality always holds and  $\zeta(\gamma)$  increases with  $\gamma$ . We conclude that if  $\gamma_1 \leq \gamma_2$ , we have  $-\frac{G_x}{G_y} \leq -\frac{H_x}{H_y}$  and, thus,  $y_c(x) > y_t(x)$ . In such a case, the minimizer is  $f^*(p, p_1, b)$ . Similarly, when  $\gamma_1 > \gamma_2$ , the minimizer is  $f^*(p, a, p_2)$ .

## APPENDIX E

The curve  $Q_1(\omega, F)$  intersects the line  $\omega = \bar{p} + \bar{P}$  at most in a single point. To prove this, we substitute  $\omega = \bar{p} + \bar{P}$  in the expression for  $Q_1(\omega, F) = 0$ , i.e., we compute  $(R_1^{\min} = \tilde{R}_2^{\max})|_{\omega=\bar{p}+\bar{P}}$  which can be conveniently rewritten as

$$-\log\left(1 - \frac{\bar{P}\beta_0}{F(1+a)}\right) = F \log\left(1 - \frac{\bar{P}\beta_0 v}{F(\beta_0 + av)}\right) + \log\left(1 + \frac{av}{\beta_0}\right) \quad (46)$$

where  $a = \beta_0(\bar{p} + \bar{P})$ . The l.h.s of (46) is defined when  $\frac{\bar{P}\beta_0}{F(1+a)} < 1$ , i.e., when  $F \geq \frac{\bar{P}\beta_0}{1+a}$ , which is always true in  $\Omega$  where  $F$  is larger than in  $V_3$ , i.e.,  $\frac{\bar{P}\beta_0}{a}$ . Moreover, the l.h.s of (46) decreases with  $F$  while the r.h.s of (46) increases with  $F$ ; thus, (46) has at most one solution.

## REFERENCES

- [1] A. El Gamal, M. Mohseni, and S. Zahedi, "Bounds on capacity and minimum energy-per-bit for AWGN relay channels," *IEEE Trans. Inf. Theory*, vol. 52, no. 4, pp. 1545–1561, Apr. 2006.
- [2] A. Zafar, M. Shaqfeh, M.-S. Alouini, and H. Alnuweiri, "Resource allocation for two source-destination pairs sharing a single relay with a buffer," *IEEE Trans. Commun.*, vol. 62, no. 5, pp. 1444–1457, May 2014.
- [3] M. Cardone, D. Tuninetti, R. Knopp, and U. Salim, "On the Gaussian half-duplex relay channel," *IEEE Trans. Inf. Theory*, vol. 60, no. 5, pp. 2542–2562, May 2014.
- [4] R. R. Thomas, M. Cardone, R. Knopp, D. Tuninetti, and B. T. Maharaj, "A practical feasibility study of a novel strategy for the Gaussian half-duplex relay channel," *IEEE Trans. Wireless Commun.*, vol. 16, no. 1, pp. 101–116, Jan. 2017.



[5] L. Wang and M. Naghshvar, "On the capacity of the noncausal relay channel," *IEEE Trans. Inf. Theory*, vol. 63, no. 6, pp. 3554–3564, Jun. 2017.

[6] G. Kramer, "Models and theory for relay channels with receive constraints," in *Proc. 42nd Annu. Allerton Conf. Commun., Control, Comput.*, Sep. 2004, pp. 1312–1321.

[7] N. Zlatanov, V. Jamali, and R. Schober, "On the capacity of the two-hop half-duplex relay channel," in *Proc. IEEE Global Commun. Conf. (GLOBECOM)*, Dec. 2015, pp. 1–7.

[8] T. Riihonen, S. Werner, and R. Wichman, "Hybrid full-duplex/half-duplex relaying with transmit power adaptation," *IEEE Trans. Wireless Commun.*, vol. 10, no. 9, pp. 3074–3085, Sep. 2011.

[9] B. P. Day, A. R. Margetts, D. W. Bliss, and P. Schniter, "Full-duplex MIMO relaying: Achievable rates under limited dynamic range," *IEEE J. Sel. Areas Commun.*, vol. 30, no. 8, pp. 1541–1553, Sep. 2012.

[10] Y. Y. Kang, B.-J. Kwak, and J. H. Cho, "An optimal full-duplex AF relay for joint analog and digital domain self-interference cancellation," *IEEE Trans. Commun.*, vol. 62, no. 8, pp. 2758–2772, Aug. 2014.

[11] A. Behboodi, A. Chaaban, R. Mathar, and M. S. Alouini, "On full duplex Gaussian relay channels with self-interference," in *Proc. IEEE Int. Symp. Inf. Theory (ISIT)*, Jul. 2016, pp. 1864–1868.

[12] N. Zlatanov, E. Sippel, V. Jamali, and R. Schober, "Capacity of the Gaussian two-hop full-duplex relay channel with residual self-interference," *IEEE Trans. Commun.*, vol. 65, no. 3, pp. 1005–1021, Mar. 2017.

[13] T. M. Cover and A. A. El Gamal, "Capacity theorems for the relay channel," *IEEE Trans. Inf. Theory*, vol. IT-25, no. 5, pp. 572–584, Sep. 1979.

[14] T. Riihonen, S. Werner, and R. Wichman, "Mitigation of loopback self-interference in full-duplex MIMO relays," *IEEE Trans. Signal Process.*, vol. 59, no. 12, pp. 5983–5993, Dec. 2011.

[15] D. Korpi, T. Riihonen, K. Haneda, K. Yamamoto, and M. Valkama, "Achievable transmission rates and self-interference channel estimation in hybrid full-duplex/half-duplex MIMO relaying," in *Proc. IEEE 82nd Veh. Technol. Conf. (VTC Fall)*, Sep. 2015, pp. 1–5.

[16] S. Li, M. Zhou, J. Wu, L. Song, Y. Li, and H. Li, "On the performance of X-duplex relaying," *IEEE Trans. Wireless Commun.*, vol. 16, no. 3, pp. 1868–1880, Mar. 2017.

[17] Y. Gu, H. Chen, Y. Li, and B. Vucetic, "Ultra-reliable short-packet communications: Half-duplex or full-duplex relaying?" *IEEE Wireless Commun. Lett.*, to be published.

[18] X. Yue, Y. Liu, S. Kang, A. Nallanathan, and Z. Ding, "Exploiting full/half-duplex user relaying in noma systems," *IEEE Trans. Commun.*, vol. 62, no. 2, pp. 560–575, Feb. 2017.

[19] C. YU, A. Shang, P. J. Smith, G. K. Woodward, and H. A. Suraweera, "Linear transceivers for full duplex MIMO relays," in *Proc. Austral. Commun. Theory Workshop (AusCTW)*, Feb. 2014, pp. 11–16.

[20] Q. Shi, M. Hong, X. Gao, E. Song, Y. Cai, and W. Xu, "Joint source-relay design for full-duplex MIMO AF relay systems," *IEEE Trans. Signal Process.*, vol. 64, no. 23, pp. 6118–6131, Dec. 2016.

[21] A. Nordio, C.-F. Chiasserini, and E. Viterbo, "Optimal transmission strategy in full-duplex relay networks," in *Proc. IEEE Inf. Theory Workshop*, Kaohsiung, Taiwan, Nov. 2017, pp. 504–508.

[22] A. Nordio, C. F. Chiasserini, and E. Viterbo. (2017). "Optimal power allocation strategies in full-duplex relay networks." [Online]. Available: <https://arxiv.org/abs/1708.01407>



**Alessandro Nordio** (S'00–M'03) received the Ph.D. degree from EPFL, Lausanne, Switzerland, in 2002. From 1999 to 2002, he was with the Department of Mobile Communications, Eurecom Institute, Sophia Antipolis, France. From 2002 to 2009, he was a Post-Doctoral Researcher with the Politecnico di Torino, Italy. He is currently a Researcher with CNR-IEIIT, Torino, Italy. His research interests are in the field of signal processing, wireless sensor networks, theory of random matrices, and crowdsourcing systems.



**Carla-Fabiana Chiasserini** (M'98–SM'09–F'18) received the Ph.D. degree from the Politecnico di Torino, Italy, in 2000. She was a Visiting Researcher at UCSD from 1998 to 2003, and a Visiting Professor at Monash University, Australia, in 2012 and 2015. She is currently an Associate Professor with the Department of Electronics and Telecommunications, Politecnico di Torino. Her research interests include architectures, protocols, and performance analysis of mobile networks.



**Emanuele Viterbo** (M'95–SM'04–F'11) received the Ph.D. degree in electrical engineering from the Politecnico di Torino, Torino, Italy, in 1995. From 1990 to 1992, he was with the European Patent Office, The Hague, The Netherlands. From 1995 to 1997, he held a post-doctoral position at the Politecnico di Torino. From 1997 to 1998, he was a Post-Doctoral Research Fellow with the Information Sciences Research Center, AT&T Research, Florham Park, NJ, USA. From 1998 to 2005, he was an Assistant Professor and then an Associate Professor, Politecnico di Torino. From 2006 to 2009, he was with the University of Calabria, Italy, as a Full Professor. He is currently a Professor with the Electrical and Computer Systems Engineering Department and an Associate Dean in graduate research with Monash University, Melbourne, Australia. He has been an ISI Highly Cited Researcher since 2009.